Electric dipole moments of baryons with bottom quarks

Y. Ünal,[1,2,*] D. Severt,[1,†] J. de Vries,[3,4,‡] C. Hanhart,[5,§] and Ulf-G. Meißner[1,5,6,‖]

[1]*Helmholtz-Institut für Strahlen- und Kernphysik and Bethe Center for Theoretical Physics, Universität Bonn, D-53115 Bonn, Germany*
[2]*Physics Department, Çanakkale Onsekiz Mart University, 17100 Çanakkale, Turkey*
[3]*Institute for Theoretical Physics Amsterdam and Delta Institute for Theoretical Physics, University of Amsterdam, Science Park 904, 1098 XH Amsterdam, Netherlands*
[4]*Nikhef, Theory Group, Science Park 105, 1098 XG Amsterdam, Netherlands*
[5]*Institute for Advanced Simulation, Institut für Kernphysik and Jülich Center for Hadron Physics, Forschungszentrum Jülich, D-52425 Jülich, Germany*
[6]*Tbilisi State University, 0186 Tbilisi, Georgia*

(Received 13 December 2021; accepted 23 February 2022; published 29 March 2022)

Triggered by experimental prospects to measure electromagnetic dipole moments of baryons containing a bottom quark, we calculate the *CP*-odd electric dipole moments (EDMs) of spin-1/2 single-bottom baryons. We consider *CP*-violating dimension-6 operators in the Standard Model effective field theory that involve bottom quarks and apply heavy-baryon chiral perturbation theory to compute the EDMs of several baryons. We discuss the expected size of the EDMs for beyond-the-Standard-Model physics appearing at the TeV scale.

DOI: 10.1103/PhysRevD.105.055026

I. INTRODUCTION

Experiments aiming to detect permanent electric dipole moments (EDMs) set strong bounds on flavor-diagonal mechanisms that simultaneously violate time-reversal (T) and parity (P) (and thus CP symmetry if we take CPT to be a good symmetry of nature). For instance, the strongest constraints on the QCD $\bar{\theta}$ term arise from measurements of the EDMs of the neutron and the ^{199}Hg atom [1,2]. In addition, EDM experiments strongly constrain possible sources of CP violation from beyond-the-Standard-Model (BSM) physics. While EDMs have been calculated in a plethora of different BSM models, BSM CP violation can be described more systematically in the framework of the Standard Model (SM) effective field theory (EFT) [3] under the reasonable assumption that the scale of BSM physics, Λ, lies well beyond the electroweak scale, $v \simeq 250$ GeV.

A lot of effort has gone into more and more accurate calculations of EDMs of systems containing first-generation valence quarks such as nucleons, nuclei, atoms, and molecules [4–8]. The associated experiments are mainly sensitive to CP-odd SMEFT operators containing light quarks (and leptons, but we will not pursue leptonic CP violation in this work). For instance, the nonobservation of a neutron EDM sets stringent limits on the electric and chromo-electric dipole moments of up and down quarks and various four-quark interactions [9]. The experimental limits are so stringent that the same experiments also indirectly constrain CP violation in interactions involving heavier quarks. For instance, a chromoelectric dipole moment of a bottom or top quark, induced at the scale Λ in some BSM theory, will in turn induce chromoelectric dipole moments of light quarks and gluons due to renormalization-group evolution to lower energies and threshold effects when the heavier quarks are integrated out. Systematic studies of the resulting indirect limits have appeared in several places in the literature; see, e.g., Refs. [10–13].

Although those indirect limits are already valuable, more direct information on CP-violating interactions involving heavy quarks would be welcome. First of all, additional observables would help in setting global constraints, leaving less room for possible cancellations among various sources. Second, as soon as a nonzero EDM is found, hopefully in the near future, additional information is needed to pin down the underlying source of CP violation. Third, while operators with heavy quarks contribute to first-generation EDMs, the contributions are loop suppressed and sometimes involve small dimensionless numbers such as Cabibbo-Kobayashi-Maskawa (CKM) matrix elements

*yaseminunal@comu.edu.tr
†severt@hiskp.uni-bonn.de
‡j.devries4@uva.nl
§c.hanhart@fz-juelich.de
‖meissner@hiskp.uni-bonn.de

or light-quark Yukawa couplings. Finally, and arguably most importantly, plans are being discussed to measure EDMs of baryons with a heavy valence quarks directly. For instance, Refs. [14–16] discuss the prospects of measuring EDMs of charm and bottom baryons. Further discussions on the mechanism of CP violation resulting from the QCD θ term in the charm baryon sector can be found in Ref. [17]. In this work, we calculate the EDMs of spin-1/2 bottom baryons in the framework of the SMEFT. In this way, we can determine what is the sensitivity of potential future measurements on the scale of BSM physics and whether different baryons have a different sensitivity to various CP-violating SMEFT operators.

This paper is organized as follows. In Sec. II, we discuss dimension-6 SMEFT CP-violating operators involving bottom quarks. In Sec. III we discuss how to match these operators to the hadronic level using chiral perturbation theory focusing on the operators most relevant for our EDM calculations. In Sec. IV, we perform the calculation of the EDMs of bottom-quark baryons at leading order for each source of CP violation. We discuss the expected sizes of EDMs in Sec. V and conclude in Sec. VI. Several appendices are devoted to technical issues.

II. CP-VIOLATING OPERATORS INVOLVING BOTTOM QUARKS

We start with listing CP-violating operators involving b quarks at the quark level. We focus on operators with at least one $\bar{b}\Gamma b$ bilinear, where Γ is a general Lorentz structure, while the remaining fields are light quarks or gauge or scalar bosons. Operators with more b-quark fields lead to suppressed EDMs of systems containing a single b valence quark in the same way as b-quark effects are suppressed in light states. We do not consider operators with just light quarks, even though they would contribute to b quark–containing baryons. The reason is that the limits on these CP-odd operators from traditional EDM experiments, such as those for the neutron EDM, are very stringent.

At low energies, right above the b-quark threshold, the effective P- and T-violating dimension-6 operators of relevance here read [3,5,18]

$$\begin{aligned}
\mathcal{L}^{(6)}_{b,\mathrm{qEDM}} &= d_b \bar{b}\sigma^{\mu\nu}\gamma_5 b F_{\mu\nu},\\
\mathcal{L}^{(6)}_{b,\mathrm{qCEDM}} &= \tilde{d}_b \bar{b}\sigma^{\mu\nu}\gamma_5\lambda^a b G^a_{\mu\nu},\\
\mathcal{L}^{(6)}_{b,4\mathrm{q}} &= i\mu_1^{ub}(\bar{u}u\bar{b}\gamma_5 b + \bar{u}\gamma_5 u\bar{b}b - \bar{b}\gamma_5 u\bar{u}b - \bar{b}u\bar{u}\gamma_5 b) + i\mu_1^{db}(\bar{d}d\bar{b}\gamma_5 b + \bar{d}\gamma_5 d\bar{b}b\\
&\quad - \bar{b}\gamma_5 d\bar{d}b - \bar{b}d\bar{d}\gamma_5 b) + i\mu_1^{sb}(\bar{s}s\bar{b}\gamma_5 b + \bar{s}\gamma_5 s\bar{b}b - \bar{b}\gamma_5 s\bar{s}b - \bar{b}s\bar{s}\gamma_5 b)\\
&\quad + i\mu_8^{ub}(\bar{u}\lambda^a u\bar{b}\gamma_5\lambda^a b + \bar{u}\gamma_5\lambda^a u\bar{b}\lambda^a b - \bar{b}\gamma_5\lambda^a u\bar{u}\lambda^a b - \bar{b}\lambda^a u\bar{u}\gamma_5\lambda^a b)\\
&\quad + i\mu_8^{db}(\bar{d}\lambda^a d\bar{b}\gamma_5\lambda^a b + \bar{d}\gamma_5\lambda^a d\bar{b}\lambda^a b - \bar{b}\gamma_5\lambda^a d\bar{d}\lambda^a b - \bar{b}\lambda^a d\bar{d}\gamma_5\lambda^a b)\\
&\quad + i\mu_8^{sb}(\bar{s}\lambda^a s\bar{b}\gamma_5\lambda^a b + \bar{s}\gamma_5\lambda^a s\bar{b}\lambda^a b - \bar{b}\gamma_5\lambda^a s\bar{s}\lambda^a b - \bar{b}\lambda^a s\bar{s}\gamma_5\lambda^a b),\\
\mathcal{L}^{(6)}_{b,4\mathrm{qLR}} &= i\nu_1^{ub}V_{ub}(\bar{b}_L\gamma_\mu u_L\bar{u}_R\gamma^\mu b_R) - i\nu_1^{ub}V^*_{ub}(\bar{b}_R\gamma_\mu u_R\bar{u}_L\gamma^\mu b_L)\\
&\quad + i\nu_8^{ub}V_{ub}(\bar{b}_L\gamma_\mu\lambda^a u_L\bar{u}_R\gamma^\mu\lambda^a b_R) - i\nu_8^{ub}V^*_{ub}(\bar{b}_R\gamma_\mu\lambda^a u_R\bar{u}_L\gamma^\mu\lambda^a b_L),
\end{aligned} \tag{1}$$

where V_{ub} is an element of the CKM matrix and $F_{\mu\nu}$ and $G^a_{\mu\nu}$ are the electromagnetic and the gluon field-strength tensors, respectively.

The bottom-quark EDM (qEDM) and bottom-quark chromo-EDM (qCEDM) operators arise from the dimension-6 operators in the SMEFT Lagrangian,

$$\begin{aligned}
\mathcal{L}_{4\mathrm{q}} &= C^{bB}(\bar{Q}_3\sigma^{\mu\nu}b_{R_b})HB_{\mu\nu} + C^{bW}(\bar{Q}_3\sigma^{\mu\nu}\tau^a b_{R_b})HW^a_{\mu\nu}\\
&\quad + C^{bG}(\bar{Q}_3\sigma^{\mu\nu}\lambda^a b_{R_b})HG^a_{\mu\nu} + \mathrm{H.c.},
\end{aligned} \tag{2}$$

where Q_3 denotes a left doublet of third-generation quarks; H is the Higgs doublet; and $B_{\mu\nu}$ and $W^a_{\mu\nu}$ denote, respectively, the $U(1)_Y$ and $SU(2)_L$ field strengths. To preserve gauge invariance, the SMEFT dipole operators involve a Higgs field in the SMEFT Lagrangian. Equation (1) is subsequent to electroweak symmetry breaking where we have replaced the Higgs field by its vacuum expectation value. The bottom qEDM arises from a linear combination of $U(1)_Y$ and $SU(2)_L$ dimension-6 dipole operators (there is in principle an associated dipole operator coupled to Z and $W^\pm$ bosons that play no role in our analysis). In most models of BSM physics, the dipoles scale with the bottom quark Yukawa, and we expect $d_b, \tilde{d}_b \sim m_b/\Lambda^2$. These dipole operators are generated in various classes of BSM physics ranging from supersymmetric scenarios [19] to two-Higgs doublet models [20] to leptoquarks [21].

The four-quark operators in $\mathcal{L}^{(6)}_{b,4\mathrm{q}}$ are induced from gauge-invariant operators of the form

$$\mathcal{L}_{4\mathrm{q}} = C^{abcd}_{4\mathrm{q}}(\bar{Q}^I_a u_{R_b})\epsilon_{IJ}(\bar{Q}^J_c d_{R_d}) + \mathrm{H.c.} + \ldots, \tag{3}$$

where the ellipsis denotes terms with additional color structure and $abcd$ are generation indices. These operators

induce $\mathcal{L}^{(6)}_{b,4q}$ for the generation indices $a = b = \{1,2\}$ and $c = d = 3$ or $a = d = 3$ and $b = c = \{1,2\}$ [the operator in Eq. (1) is associated to the former generation configuration; the second configuration leads to very similar low-energy operators and the analysis presented here will be the same] and additional operators involving top quarks that play no role at low energies. We expect $\mu^{ub,db,sb}_{1,8} \sim 1/\Lambda^2$. For instance, the CP-odd four-quark operators are induced in models of leptoquarks, in which case Λ is related to the mass of the exchange leptoquark [21].

The four-quark operators in $\mathcal{L}^{(6)}_{b,4qLR}$ are induced from the gauge-invariant operator

$$\mathcal{L}_{4\mathrm{qLR}} = C^{ab}_{4\mathrm{qLR}}(\tilde{H}^\dagger D_\mu H)\bar{u}^a_R\gamma^\mu b^b_R + \mathrm{H.c.}. \tag{4}$$

After electroweak symmetry breaking, this operator leads to a right-handed charged current. The interactions in $\mathcal{L}^{(6)}_{b,4qLR}$ are generated when the W boson is integrated out at tree level between quarks, giving rise to the additional factor of V_{ub}. By power counting, $\nu^{ub}_{1,8} \sim v^2/(m_W^2\Lambda^2) \sim 1/\Lambda^2$. An example where this operator is generated is the minimal left-right symmetric model [9].

III. CHIRAL PERTURBATION THEORY FOR BOTTOM BARYONS

The way to include heavy bottom quarks into standard chiral perturbation theory (ChPT) has been known for some time [22,23]. In the SU(3) flavor representation, the spin-1/2 antisymmetric triplet and symmetric sextet bottom baryon states are denoted by the following matrices, respectively:

$$B_{\bar{3}} = \begin{pmatrix} 0 & \Lambda_b^0 & \Xi_b^0 \\ -\Lambda_b^0 & 0 & \Xi_b^- \\ -\Xi_b^0 & -\Xi_b^- & 0 \end{pmatrix}, \quad B_6 = \begin{pmatrix} \Sigma_b^+ & \frac{\Sigma_b^0}{\sqrt{2}} & \frac{\Xi_b'^0}{\sqrt{2}} \\ \frac{\Sigma_b^0}{\sqrt{2}} & \Sigma_b^- & \frac{\Xi_b'^-}{\sqrt{2}} \\ \frac{\Xi_b'^0}{\sqrt{2}} & \frac{\Xi_b'^-}{\sqrt{2}} & \Omega_b^- \end{pmatrix}. \tag{5}$$

The Goldstone boson octet is given by

$$\phi = \begin{pmatrix} \frac{1}{\sqrt{2}}\pi^0 + \frac{1}{\sqrt{6}}\eta & \pi^+ & K^+ \\ \pi^- & -\frac{1}{\sqrt{2}}\pi^0 + \frac{1}{\sqrt{6}}\eta & K^0 \\ K^- & \bar{K}^0 & -\frac{2}{\sqrt{6}}\eta \end{pmatrix}, \tag{6}$$

and we define

$$U = u^2 = \exp\left(i\frac{\phi}{F_\pi}\right), \tag{7}$$

where F_π is the pion decay constant. The relevant P- and T-conserving free and interaction Lagrangians up to the second chiral order in a covariant formalism are given by [23–26]

$$\begin{aligned}
\mathcal{L}^{(1)}_{\mathrm{free}} &= \frac{1}{2}\langle\bar{B}_{\bar{3}}(i\not{D} - m_{\bar{3}})B_{\bar{3}}\rangle + \langle\bar{B}_6(i\not{D} - m_6)B_6\rangle, \\
\mathcal{L}_{\mathrm{int}} &= \frac{g_1}{2}\langle\bar{B}_6\not{u}\gamma_5 B_6\rangle + \frac{g_2}{2}\langle\bar{B}_6\not{u}\gamma_5 B_{\bar{3}} + \mathrm{H.c.}\rangle + \frac{g_3}{2}\langle\bar{B}_{\bar{3}}\not{u}\gamma_5 B_{\bar{3}}\rangle, \\
\mathcal{L}^{(2)}_{B\gamma} &= w_1\langle\bar{B}_{\bar{3}}\sigma^{\mu\nu}F^+_{\mu\nu}B_{\bar{3}}\rangle + w_2\langle\bar{B}_6\sigma^{\mu\nu}F^+_{\mu\nu}B_6\rangle \\
&\quad + w_3\langle\bar{B}_6\sigma^{\mu\nu}F^+_{\mu\nu}B_3 + \mathrm{H.c.}\rangle + w_4\langle\bar{B}_{\bar{3}}\sigma^{\mu\nu}B_{\bar{3}}\rangle\langle F^+_{\mu\nu}\rangle \\
&\quad + w_5\langle\bar{B}_6\sigma^{\mu\nu}B_6\rangle\langle F^+_{\mu\nu}\rangle.
\end{aligned} \tag{8}$$

Here, D_μ is the covariant derivative defined as

$$\begin{aligned}
D_\mu B &= \partial_\mu B + \Gamma_\mu B + B\Gamma^T_\mu, \\
\Gamma_\mu &= \frac{1}{2}[u^\dagger(\partial_\mu - ir_\mu)u + u(\partial_\mu - il_\mu)u^\dagger],
\end{aligned} \tag{9}$$

and u_μ is the standard chiral Vielbein

$$u_\mu = i[u^\dagger(\partial_\mu - ir_\mu)u - u(\partial_\mu - il_\mu)u^\dagger], \tag{10}$$

where r_μ and l_μ denote external right- and left-handed sources. Also, we have

$$F^+_{\mu\nu} = u^\dagger Q_B F_{\mu\nu} u + u Q_B F_{\mu\nu} u^\dagger, \tag{11}$$

with the bottom baryon charge matrix [27]

$$Q_B = \frac{e}{2}\mathrm{diag}(1,-1,-1). \tag{12}$$

The prefactors g_{1-3} and w_{1-5} are low-energy constants (LECs). g_2 is calculated using the widths of the heavy baryons. g_1 and g_3 are related to g_2 with the help of the quark model and heavy-quark spin flavor symmetry [23,25,27,28]. Because of the heavy-quark spin symmetry, the vertex $B_{\bar{3}}B_{\bar{3}}\phi$ is forbidden, and the term has to vanish, i.e., $g_3 = 0$. This result can be deduced from angular momentum and parity conservation arguments (see, e.g., Ref. [23]). The conventional magnetic moment couplings, w_{1-5}, are determined from fits to calculations to baryon magnetic moments in Refs. [29,30]. However, in the present calculation, they do not contribute to the EDMs at the order at which we work. The numerical values of the contributing couplings are given in Sec. V.

A. Construction of the effective *CP*-violating Lagrangian

We now turn to the construction of the effective Lagrangian on the hadron level arising from the dimension-6 terms in Eq. (1). The first operator we want to look at is the qEDM, which does not contain any light quarks but only the heavy b quark. As it already contains the electromagnetic field strength tensor $F_{\mu\nu}$, it directly

induces EDMs of baryons containing bottom quarks. We find only two terms in the leading chiral Lagrangian corresponding to EDMs of the antitriplet and sextet of bottom-quark baryons.

Next, we discuss the qCEDM. Similarly to the qEDM, there is no light-quark content in the Lagrangian, and instead of $F_{\mu\nu}$, we have the gluon field strength tensor $G^a_{\mu\nu}$. The fact that this term contains only heavy quarks and $G^a_{\mu\nu}$ makes this term (like the qEDM) a chiral singlet; i.e., it is invariant under chiral SU(3) transformations. In standard ChPT, there is no fundamental building block that transforms as a chiral singlet. Therefore, we have to introduce a new fundamental block β^+, which gives the proper transformation behavior, and a partner building block β^-, which transforms accordingly and explicitly violates P and T. This procedure works analogously to the definition of the building blocks χ_+ and χ_- in ChPT. However, in contrast to the building blocks $\chi_\pm$, the chiral singlet β^+ cannot introduce any further structure containing Goldstone boson fields. In fact, it can be shown that β^+ can only enter the effective Lagrangian as an overall constant. In a similar fashion, one can also deduce that a P- and T-violating chiral singlet term β^- will always vanish. There is simply no constant that can violate P and T. Despite β^+ being a constant, we still have to treat it like a building block. To construct the effective Lagrangian on the hadron level, we need to combine β^+ with other ChPT building blocks that violate CP This procedure leads to the terms given below. For more information, see, e.g., Refs. [6,18].

The next contributions we investigate are the four quark interaction terms (4q operators). These terms need a little extra treatment, since they not just include the heavy bottom quark but also the light quarks u, d, and s. Because of the presence of the light quarks, we have to study how the 4q terms transform under chiral transformations. To obtain the transformation properties of $\mathcal{L}^{(6)}_{b,4q}$ under chiral SU(3) transformations, we first express the nonmixing μ_1 terms of the operator as follows:

$$i\mu_1^{ub}(\bar{u}u\bar{b}\gamma_5 b + \bar{u}\gamma_5 u\bar{b}b) + i\mu_1^{db}(\bar{d}d\bar{b}\gamma_5 b + \bar{d}\gamma_5 d\bar{b}b) + i\mu_1^{sb}(\bar{s}s\bar{b}\gamma_5 b + \bar{s}\gamma_5 s\bar{b}b). \tag{13}$$

These terms have the structure

$$i\bar{q}\mathcal{M}_1 q(\bar{b}\gamma_5 b) + i\bar{q}\mathcal{M}_1\gamma_5 q(\bar{b}b), \tag{14}$$

in terms of the quark column vector $q = (u, d, s)^T$ and

$$\mathcal{M}_1 = \begin{pmatrix} \mu_1^{ub} & 0 & 0 \\ 0 & \mu_1^{db} & 0 \\ 0 & 0 & \mu_1^{sb} \end{pmatrix}. \tag{15}$$

For the light quarks, Eq. (14) has the structure of a mass term in ordinary ChPT because the term containing the b quarks is a SU(3) singlet and does not transform at all. The $\mathcal{M}_1$ matrix will therefore act as a new scalar source, similar to the quark mass matrix in standard ChPT, while the explicit insertions of the b-quark field allow for the appearance of the heavy bottom baryon matrices $B_{\bar{3}}$ and B_6 in the effective Lagrangian.

The mixing terms in the 4q Lagrangian,

$$-i\mu_1^{ub}(\bar{b}\gamma_5 u\bar{u}b + \bar{b}u\bar{u}\gamma_5 b) - i\mu_1^{db}(\bar{b}\gamma_5 d\bar{d}b + \bar{b}d\bar{d}\gamma_5 b) - i\mu_1^{sb}(\bar{b}\gamma_5 s\bar{s}b + \bar{b}s\bar{s}\gamma_5 b), \tag{16}$$

can be treated in an analogous way. If we use the identities

$$\bar{q}q = \bar{u}u + \bar{d}d + \bar{s}s, \qquad q\bar{q} = \begin{pmatrix} u\bar{u} & u\bar{d} & u\bar{s} \\ d\bar{u} & d\bar{d} & d\bar{s} \\ s\bar{u} & s\bar{d} & s\bar{s} \end{pmatrix}, \qquad \langle q\bar{q}\rangle = u\bar{u} + d\bar{d} + s\bar{s}, \tag{17}$$

we can express Eq. (16) together with Eqs. (15) and (17) as

$$-i\bar{b}\gamma_5\langle(\mathcal{M}_1 q)\bar{q}\rangle b - i\bar{b}\langle(\mathcal{M}_1 q)\bar{q}\rangle\gamma_5 b. \tag{18}$$

Using the cyclic property of the trace, one observes that these mixing terms transform again like a mass term. Thus, we can use the same procedure like in the nonmixing case to obtain the effective Lagrangian.

For the 4q operators, the μ_1 and μ_8 terms have identical chiral symmetry properties. While these terms are distinguishable on the quark level, at low energies, the resulting chiral Lagrangians are identical. We are not able to distinguish them without nonperturbative information about the associated low-energy constants. The effective Lagrangian from the $4q$ operator will therefore combine the effects of the μ_1 and μ_8 terms.

The last terms we have to discuss are the four quark left-right operator (4qLR) terms. Similarly to the 4q operator, one can reproduce the transformation rules for the 4qLR operator. First, we take the ν_1^{ub} terms and use Fierz identities to rewrite the left- and right-handed components of the quark fields. Then, we arrange the resulting terms, like before, in structures involving the quark vector q and a new scalar source,

$$\mathcal{N}_1 = \begin{pmatrix} \nu_1^{ub} & 0 & 0 \\ 0 & 0 & 0 \\ 0 & 0 & 0 \end{pmatrix}. \tag{19}$$

We find the same transformation behavior as for the 4q case. This leads to an identical EFT Lagrangian construction procedure. Also, here, the 4qLR terms involving the constant ν_8^{ub} are not distinguishable from the ν_1^{ub} terms at the level of chiral EFT. Finally, we mention that

after rewriting the terms with Fierz identities we obtain both P- and T-violating and P- and T-conserving interactions. The latter lead to modifications of P- and T-even observables that are swamped by Standard Model contributions, and we neglect them below.

We are now in the position to write down the hadronic Lagrangians accounting for the various P- and T-violating dimension-6 operators. For the quark EDM, we obtain the two operators

$$\mathcal{L}^{\rm eff}_{\rm qEDM} = c_1\langle \bar{B}_{\bar{3}}\sigma^{\mu\nu}\gamma_5 F_{\mu\nu}B_{\bar{3}}\rangle + c_2\langle \bar{B}_6\sigma^{\mu\nu}\gamma_5 F_{\mu\nu}B_6\rangle + \ldots. \tag{20}$$

A much longer list of operators appears for the qCEDM. Here, we give all operators that appear at the same chiral order. As discussed below, not all operators are relevant for the EDM calculations we perform. We list them here for completeness. These read

$$\begin{aligned}
\mathcal{L}^{\rm eff}_{\rm qCEDM} = {} & i\beta^+[b_1\langle \bar{B}_{\bar{3}}\chi_+\gamma_5 B_{\bar{3}}\rangle + b_2\langle \bar{B}_6\chi_+\gamma_5 B_6\rangle + b_3\langle \bar{B}_6\chi_+\gamma_5 B_{\bar{3}} + \text{H.c.}\rangle + b_4\langle \bar{B}_{\bar{3}}\gamma_5 B_{\bar{3}}\rangle\langle\chi_+\rangle \\
& + b_5\langle \bar{B}_6\gamma_5 B_6\rangle\langle\chi_+\rangle + b_6\langle \bar{B}_{\bar{3}}\chi_- B_{\bar{3}}\rangle + b_7\langle \bar{B}_6\chi_- B_6\rangle + b_8\langle \bar{B}_6\chi_- B_{\bar{3}} + \text{H.c.}\rangle + b_9\langle \bar{B}_{\bar{3}}B_{\bar{3}}\rangle\langle\chi_-\rangle \\
& + b_{10}\langle \bar{B}_6 B_6\rangle\langle\chi_-\rangle] + i\beta^+[b_{11}\langle \bar{B}_{\bar{3}}u^\mu\gamma_5 u_\mu B_{\bar{3}}\rangle + b_{12}\langle \bar{B}_6 u^\mu\gamma_5 u_\mu B_6\rangle + b_{13}\langle \bar{B}_6 u^\mu\gamma_5 u_\mu B_{\bar{3}} + \text{H.c.}\rangle \\
& + b_{14}\langle \bar{B}_{\bar{3}}\gamma_5 B_{\bar{3}}\rangle\langle u^\mu u_\mu\rangle + b_{15}\langle \bar{B}_6\gamma_5 B_6\rangle\langle u^\mu u_\mu\rangle] + \beta^+[b_{16}\langle \bar{B}_{\bar{3}}\sigma^{\mu\nu}\gamma_5 F^+_{\mu\nu}B_{\bar{3}}\rangle + b_{17}\langle \bar{B}_6\sigma^{\mu\nu}\gamma_5 F^+_{\mu\nu}B_6\rangle \\
& + b_{18}\langle \bar{B}_6\sigma^{\mu\nu}\gamma_5 F^+_{\mu\nu}B_{\bar{3}} + \text{H.c.}\rangle + b_{19}\langle \bar{B}_{\bar{3}}\sigma^{\mu\nu}\gamma_5 B_{\bar{3}}\rangle\langle F^+_{\mu\nu}\rangle + b_{20}\langle \bar{B}_6\sigma^{\mu\nu}\gamma_5 B_6\rangle\langle F^+_{\mu\nu}\rangle] \\
& + \beta^+[b_{21}\langle \bar{B}_{\bar{3}}\sigma^{\mu\nu}\gamma_5[u_\mu,u_\nu]B_{\bar{3}}\rangle + b_{22}\langle \bar{B}_6\sigma^{\mu\nu}\gamma_5[u_\mu,u_\nu]B_6\rangle + b_{23}\langle \bar{B}_6\sigma^{\mu\nu}\gamma_5[u_\mu,u_\nu]B_{\bar{3}} + \text{H.c.}\rangle] \\
& + \beta^+[b_{24}\langle \bar{B}_{\bar{3}}u^\mu\rangle\langle u^\nu\sigma_{\mu\nu}\gamma_5 B_{\bar{3}}\rangle + b_{25}\langle \bar{B}_6 u^\mu\rangle\langle u^\nu\sigma_{\mu\nu}\gamma_5 B_6\rangle + b_{26}\langle \bar{B}_6 u^\mu\rangle\langle u^\nu\sigma_{\mu\nu}\gamma_5 B_{\bar{3}}\rangle + \text{H.c.}] \\
& + i\beta^+[b_{27}\langle \bar{B}_{\bar{3}}u^\mu u^\nu\gamma_\mu\gamma_5 D_\nu B_{\bar{3}}\rangle - b_{28}\langle \bar{B}_{\bar{3}}\overleftarrow{D}_\nu u^\mu u^\nu\gamma_\mu\gamma_5 B_{\bar{3}}\rangle + b_{29}\langle \bar{B}_6 u^\mu u^\nu\gamma_\mu\gamma_5 D_\nu B_6\rangle \\
& - b_{30}\langle \bar{B}_6\overleftarrow{D}_\nu u^\mu u^\nu\gamma_\mu\gamma_5 B_6\rangle + b_{31}\langle \bar{B}_6 u^\mu u^\nu\gamma_\mu\gamma_5 D_\nu B_{\bar{3}} + \text{H.c.}\rangle - b_{32}\langle \bar{B}_6\overleftarrow{D}_\nu u^\mu u^\nu\gamma_\mu\gamma_5 B_{\bar{3}} + \text{H.c.}\rangle] \\
& + i\beta^+[(b_{33}\langle \bar{B}_{\bar{3}}\gamma^\mu\gamma_5 D^\nu B_{\bar{3}}\rangle - b_{34}\langle \bar{B}_{\bar{3}}\overleftarrow{D}^\nu\gamma^\mu\gamma_5 B_{\bar{3}}\rangle)\langle u_\mu u_\nu\rangle + (b_{35}\langle \bar{B}_6\gamma^\mu\gamma_5 D^\nu B_6\rangle \\
& - b_{36}\langle \bar{B}_6\overleftarrow{D}^\nu\gamma^\mu\gamma_5 B_6\rangle)\langle u_\mu u_\nu\rangle + (b_{37}\langle \bar{B}_6\gamma^\mu\gamma_5 D^\nu B_{\bar{3}} + \text{H.c.}\rangle - b_{38}\langle \bar{B}_6\overleftarrow{D}^\nu\gamma^\mu\gamma_5 B_{\bar{3}} + \text{H.c.}\rangle)\langle u_\mu u_\nu\rangle] + \ldots.
\end{aligned} \tag{21}$$

For the four-quark operators, we obtain

$$\begin{aligned}
\mathcal{L}^{\rm eff}_{\rm 4q} = {} & i\mu_1\langle \bar{B}_{\bar{3}}\tilde{\chi}_+\gamma_5 B_{\bar{3}}\rangle + i\mu_2\langle \bar{B}_6\tilde{\chi}_+\gamma_5 B_6\rangle + i\mu_3\langle \bar{B}_6\tilde{\chi}_+\gamma_5 B_{\bar{3}} + \text{H.c.}\rangle + i\mu_4\langle \bar{B}_{\bar{3}}\gamma_5 B_{\bar{3}}\rangle\langle\tilde{\chi}_+\rangle \\
& + i\mu_5\langle \bar{B}_6\gamma_5 B_6\rangle\langle\tilde{\chi}_+\rangle + i\mu_6\langle \bar{B}_{\bar{3}}\tilde{\chi}_- B_{\bar{3}}\rangle + i\mu_7\langle \bar{B}_6\tilde{\chi}_- B_6\rangle + i\mu_8\langle \bar{B}_6\tilde{\chi}_- B_{\bar{3}} + \text{H.c.}\rangle \\
& + i\mu_9\langle \bar{B}_{\bar{3}}B_{\bar{3}}\rangle\langle\tilde{\chi}_-\rangle + i\mu_{10}\langle \bar{B}_6 B_6\rangle\langle\tilde{\chi}_-\rangle + \mu_{11}\langle \bar{B}_{\bar{3}}\tilde{\chi}_+\sigma^{\mu\nu}\gamma_5 F^+_{\mu\nu}B_{\bar{3}}\rangle + \mu_{12}\langle \bar{B}_6\tilde{\chi}_+\sigma^{\mu\nu}\gamma_5 F^+_{\mu\nu}B_6\rangle \\
& + \mu_{13}\langle \bar{B}_6\tilde{\chi}_+\sigma^{\mu\nu}\gamma_5 F^+_{\mu\nu}B_{\bar{3}} + \text{H.c.}\rangle + \mu_{14}\langle \bar{B}_{\bar{3}}\tilde{\chi}_+\sigma^{\mu\nu}\gamma_5 B_{\bar{3}}\rangle\langle F^+_{\mu\nu}\rangle + \mu_{15}\langle \bar{B}_6\tilde{\chi}_+\sigma^{\mu\nu}\gamma_5 B_6\rangle\langle F^+_{\mu\nu}\rangle \\
& + \mu_{16}\langle \bar{B}_6\tilde{\chi}_+\sigma^{\mu\nu}\gamma_5 B_{\bar{3}} + \text{H.c.}\rangle\langle F^+_{\mu\nu}\rangle + \mu_{17}\langle \bar{B}_{\bar{3}}\sigma^{\mu\nu}\gamma_5 F^+_{\mu\nu}B_{\bar{3}}\rangle\langle\tilde{\chi}_+\rangle + \mu_{18}\langle \bar{B}_6\sigma^{\mu\nu}\gamma_5 F^+_{\mu\nu}B_6\rangle\langle\tilde{\chi}_+\rangle \\
& + \mu_{19}\langle \bar{B}_6\sigma^{\mu\nu}\gamma_5 F^+_{\mu\nu}B_{\bar{3}} + \text{H.c.}\rangle\langle\tilde{\chi}_+\rangle + \mu_{20}\langle \bar{B}_{\bar{3}}\sigma^{\mu\nu}\gamma_5 B_{\bar{3}}\rangle\langle\tilde{\chi}_+ F^+_{\mu\nu}\rangle + \mu_{21}\langle \bar{B}_6\sigma^{\mu\nu}\gamma_5 B_6\rangle\langle\tilde{\chi}_+ F^+_{\mu\nu}\rangle \\
& + \mu_{22}\langle \bar{B}_{\bar{3}}\tilde{\chi}_-\sigma^{\mu\nu}F^+_{\mu\nu}B_{\bar{3}}\rangle + \mu_{23}\langle \bar{B}_6\tilde{\chi}_-\sigma^{\mu\nu}F^+_{\mu\nu}B_6\rangle + \mu_{24}\langle \bar{B}_6\tilde{\chi}_-\sigma^{\mu\nu}F^+_{\mu\nu}B_{\bar{3}} + \text{H.c.}\rangle \\
& + \mu_{25}\langle \bar{B}_{\bar{3}}\tilde{\chi}_-\sigma^{\mu\nu}B_{\bar{3}}\rangle\langle F^+_{\mu\nu}\rangle + \mu_{26}\langle \bar{B}_6\tilde{\chi}_-\sigma^{\mu\nu}B_6\rangle\langle F^+_{\mu\nu}\rangle + \mu_{27}\langle \bar{B}_6\tilde{\chi}_-\sigma^{\mu\nu}B_{\bar{3}} + \text{H.c.}\rangle\langle F^+_{\mu\nu}\rangle \\
& + \mu_{28}\langle \bar{B}_{\bar{3}}\sigma^{\mu\nu}F^+_{\mu\nu}B_{\bar{3}}\rangle\langle\tilde{\chi}_-\rangle + \mu_{29}\langle \bar{B}_6\sigma^{\mu\nu}F^+_{\mu\nu}B_6\rangle\langle\tilde{\chi}_-\rangle + \mu_{30}\langle \bar{B}_6\sigma^{\mu\nu}F^+_{\mu\nu}B_{\bar{3}} + \text{H.c.}\rangle\langle\tilde{\chi}_-\rangle \\
& + \mu_{31}\langle \bar{B}_{\bar{3}}\sigma^{\mu\nu}B_{\bar{3}}\rangle\langle\tilde{\chi}_- F^+_{\mu\nu}\rangle + \mu_{32}\langle \bar{B}_6\sigma^{\mu\nu}B_6\rangle\langle\tilde{\chi}_- F^+_{\mu\nu}\rangle + \ldots
\end{aligned} \tag{22}$$

and

$$\begin{aligned}
\mathcal{L}^{\rm eff}_{\rm 4qLR} = {} & i\text{Re}(V_{ub})[\nu_1\langle \bar{B}_{\bar{3}}\hat{\tilde{\chi}}_- B_{\bar{3}}\rangle + \nu_2\langle \bar{B}_6\hat{\tilde{\chi}}_- B_6\rangle + \nu_3\langle \bar{B}_6\hat{\tilde{\chi}}_- B_{\bar{3}} + \text{H.c.}\rangle + \nu_4\langle \bar{B}_{\bar{3}}B_{\bar{3}}\rangle\langle\hat{\tilde{\chi}}_-\rangle \\
& + \nu_5\langle \bar{B}_6 B_6\rangle\langle\hat{\tilde{\chi}}_-\rangle + \nu_6\langle \bar{B}_{\bar{3}}\hat{\tilde{\chi}}_+\gamma_5 B_{\bar{3}}\rangle + \nu_7\langle \bar{B}_6\hat{\tilde{\chi}}_+\gamma_5 B_6\rangle + \nu_8\langle \bar{B}_6\hat{\tilde{\chi}}_+\gamma_5 B_{\bar{3}} + \text{H.c.}\rangle \\
& + \nu_9\langle \bar{B}_{\bar{3}}\gamma_5 B_{\bar{3}}\rangle\langle\hat{\tilde{\chi}}_+\rangle + \nu_{10}\langle \bar{B}_6\gamma_5 B_6\rangle\langle\hat{\tilde{\chi}}_+\rangle] + \text{Re}(V_{ub})[\nu_{11}\langle \bar{B}_{\bar{3}}\hat{\tilde{\chi}}_+\sigma^{\mu\nu}\gamma_5 F^+_{\mu\nu}B_{\bar{3}}\rangle \\
& + \nu_{12}\langle \bar{B}_6\hat{\tilde{\chi}}_+\sigma^{\mu\nu}\gamma_5 F^+_{\mu\nu}B_6\rangle + \nu_{13}\langle \bar{B}_6\hat{\tilde{\chi}}_+\sigma^{\mu\nu}\gamma_5 F^+_{\mu\nu}B_{\bar{3}} + \text{H.c.}\rangle + \nu_{14}\langle \bar{B}_{\bar{3}}\hat{\tilde{\chi}}_+\sigma^{\mu\nu}\gamma_5 B_{\bar{3}}\rangle\langle F^+_{\mu\nu}\rangle \\
& + \nu_{15}\langle \bar{B}_6\hat{\tilde{\chi}}_+\sigma^{\mu\nu}\gamma_5 B_6\rangle\langle F^+_{\mu\nu}\rangle + \nu_{16}\langle \bar{B}_6\hat{\tilde{\chi}}_+\sigma^{\mu\nu}\gamma_5 B_{\bar{3}} + \text{H.c.}\rangle\langle F^+_{\mu\nu}\rangle + \nu_{17}\langle \bar{B}_{\bar{3}}\sigma^{\mu\nu}\gamma_5 F^+_{\mu\nu}B_{\bar{3}}\rangle\langle\hat{\tilde{\chi}}_+\rangle
\end{aligned}$$

$$
\begin{aligned}
&+\nu_{18}\langle\bar{B}_6\sigma^{\mu\nu}\gamma_5 F^+_{\mu\nu}B_6\rangle\langle\hat{\tilde{\chi}}_+\rangle+\nu_{19}\langle\bar{B}_6\sigma^{\mu\nu}\gamma_5 F^+_{\mu\nu}B_{\bar{3}}+\text{H.c.}\rangle\langle\hat{\tilde{\chi}}_+\rangle+\nu_{20}\langle\bar{B}_{\bar{3}}\sigma^{\mu\nu}\gamma_5 B_{\bar{3}}\rangle\langle\hat{\tilde{\chi}}_+F^+_{\mu\nu}\rangle\\
&+\nu_{21}\langle\bar{B}_6\sigma^{\mu\nu}\gamma_5 B_6\rangle\langle\hat{\tilde{\chi}}_+F^+_{\mu\nu}\rangle+\nu_{22}\langle\bar{B}_{\bar{3}}\hat{\tilde{\chi}}_-\sigma^{\mu\nu}F^+_{\mu\nu}B_{\bar{3}}\rangle+\nu_{23}\langle\bar{B}_6\hat{\tilde{\chi}}_-\sigma^{\mu\nu}F^+_{\mu\nu}B_6\rangle\\
&+\nu_{24}\langle\bar{B}_6\hat{\tilde{\chi}}_-\sigma^{\mu\nu}F^+_{\mu\nu}B_{\bar{3}}+\text{H.c.}\rangle+\nu_{25}\langle\bar{B}_{\bar{3}}\hat{\tilde{\chi}}_-\sigma^{\mu\nu}B_{\bar{3}}\rangle\langle F^+_{\mu\nu}\rangle+\nu_{26}\langle\bar{B}_6\hat{\tilde{\chi}}_-\sigma^{\mu\nu}B_6\rangle\langle F^+_{\mu\nu}\rangle\\
&+\nu_{27}\langle\bar{B}_6\hat{\tilde{\chi}}_-\sigma^{\mu\nu}B_{\bar{3}}+\text{H.c.}\rangle\langle F^+_{\mu\nu}\rangle+\nu_{28}\langle\bar{B}_{\bar{3}}\sigma^{\mu\nu}F^+_{\mu\nu}B_{\bar{3}}\rangle\langle\hat{\tilde{\chi}}_-\rangle+\nu_{29}\langle\bar{B}_6\sigma^{\mu\nu}F^+_{\mu\nu}B_6\rangle\langle\hat{\tilde{\chi}}_-\rangle\\
&+\nu_{30}\langle\bar{B}_6\sigma^{\mu\nu}F^+_{\mu\nu}B_{\bar{3}}+\text{H.c.}\rangle\langle\hat{\tilde{\chi}}_-\rangle+\nu_{31}\langle\bar{B}_{\bar{3}}\sigma^{\mu\nu}B_{\bar{3}}\rangle\langle\hat{\tilde{\chi}}_-F^+_{\mu\nu}\rangle+\nu_{32}\langle\bar{B}_6\sigma^{\mu\nu}B_6\rangle\langle\hat{\tilde{\chi}}_-F^+_{\mu\nu}\rangle]+\ldots. \qquad (23)
\end{aligned}
$$

The ellipses indicate further terms of higher chiral order, which we will not display. We have defined

$$
\begin{aligned}
\chi_\pm &= u^\dagger\chi u^\dagger \pm u\chi^\dagger u, \qquad \chi = 2B_0\text{diag}(m_u,m_d,m_s),\\
\tilde{\chi}_\pm &= u^\dagger\tilde{\chi}u^\dagger \pm u\tilde{\chi}^\dagger u, \qquad \tilde{\chi}\equiv\text{diag}(\mu^{ub},\mu^{db},\mu^{sb}),\\
\hat{\tilde{\chi}}_\pm &= u^\dagger\hat{\tilde{\chi}}u^\dagger \pm u\hat{\tilde{\chi}}^\dagger u, \qquad \hat{\tilde{\chi}}\equiv\text{diag}(\nu^{ub},0,0), \qquad (24)
\end{aligned}
$$

with the light-quark masses m_q and the LEC B_0 related to the quark condensate. Note that the constants μ^{ub}, μ^{db}, μ^{sb}, and ν^{ub} capture both the color-singlet and -octet terms whose chiral Lagrangians are identical.

It is convenient to use heavy-baryon chiral perturbation theory (HBChPT) while working with objects that contain a single heavy quark [31,32]. In the heavy-baryon formulation, several terms in the relativistic form cancel or appear at higher orders, and loop calculations are simplified. Furthermore, the chiral power counting is manifest. The heavy-baryon Lagrangians are given by

$$
\begin{aligned}
\mathcal{L}^{(1)}_{\text{free}} &= \frac{1}{2}\langle\bar{B}_{\bar{3},v}(iv\cdot D)B_{\bar{3},v}\rangle+\langle\bar{B}_{6,v}(iv\cdot D-\Delta)B_{6,v}\rangle,\\
\mathcal{L}_{\text{int}} &= g_1\langle\bar{B}_{6,v}u_\mu S^\mu B_{6,v}\rangle+g_2\langle\bar{B}_{6,v}u_\mu S^\mu B_{\bar{3},v}+\text{H.c.}\rangle,\\
\mathcal{L}^{(2)}_{B\gamma} &= 2\varepsilon^{\mu\nu\rho\sigma}[w_1\langle\bar{B}_{\bar{3},v}v_\rho S_\sigma F^+_{\mu\nu}B_{\bar{3},v}\rangle+w_2\langle\bar{B}_{6,v}v_\rho S_\sigma F^+_{\mu\nu}B_{6,v}\rangle\\
&\quad+w_3\langle\bar{B}_{6,v}v_\rho S_\sigma F^+_{\mu\nu}B_{\bar{3},v}+\text{H.c.}\rangle\\
&\quad+w_4\langle\bar{B}_{\bar{3},v}v_\rho S_\sigma B_{\bar{3},v}\rangle\langle F^+_{\mu\nu}\rangle+w_5\langle\bar{B}_{6,v}v_\rho S_\sigma B_{6,v}\rangle\langle F^+_{\mu\nu}\rangle], \qquad (25)
\end{aligned}
$$

with the 4-velocity v^μ, the Pauli-Lubanski spin operator $S^\mu=-\gamma_5(\gamma^\mu\not{v}-v^\mu)/2$, and the mass difference between sextet and antitriplet baryons $\Delta=m_6-m_{\bar{3}}$. The effective Lagrangians for the P- and T-odd interactions in the heavy-baryon formulation are

$$
\begin{aligned}
\mathcal{L}^{\text{eff}}_{\text{qEDM}} &= 4i[c_1\langle\bar{B}_{\bar{3},v}v^\mu S^\nu F_{\mu\nu}B_{\bar{3},v}\rangle+c_2\langle\bar{B}_{6,v}v^\mu S^\nu F_{\mu\nu}B_{6,v}\rangle],\\
\mathcal{L}^{\text{eff}}_{\text{qCEDM}} &= 4i\beta^+[b_{16}\langle\bar{B}_{\bar{3},v}v^\mu S^\nu F^+_{\mu\nu}B_{\bar{3},v}\rangle+b_{17}\langle\bar{B}_{6,v}v^\mu S^\nu F^+_{\mu\nu}B_{6,v}\rangle+b_{18}\langle\bar{B}_{6,v}v^\mu S^\nu F^+_{\mu\nu}B_{\bar{3},v}+\text{H.c.}\rangle\\
&\quad+b_{19}\langle\bar{B}_{\bar{3},v}v^\mu S^\nu B_{\bar{3},v}\rangle\langle F^+_{\mu\nu}\rangle+b_{20}\langle\bar{B}_{6,v}v^\mu S^\nu B_{6,v}\rangle\langle F^+_{\mu\nu}\rangle]+\ldots,\\
\mathcal{L}^{\text{eff}}_{\text{4q}} &= i\mu_6\langle\bar{B}_{\bar{3},v}\tilde{\chi}_-B_{\bar{3},v}\rangle+i\mu_7\langle\bar{B}_{6,v}\tilde{\chi}_-B_{6,v}\rangle+i\mu_8\langle\bar{B}_{6,v}\tilde{\chi}_-B_{\bar{3},v}+\text{H.c.}\rangle+i\mu_9\langle\bar{B}_{\bar{3},v}B_{\bar{3},v}\rangle\langle\tilde{\chi}_-\rangle\\
&\quad+i\mu_{10}\langle\bar{B}_{6,v}B_{6,v}\rangle\langle\tilde{\chi}_-\rangle+4i[\mu_{11}\langle\bar{B}_{\bar{3},v}\tilde{\chi}_+v^\mu S^\nu F^+_{\mu\nu}B_{\bar{3},v}\rangle+\mu_{12}\langle\bar{B}_{6,v}\tilde{\chi}_+v^\mu S^\nu F^+_{\mu\nu}B_{6,v}\rangle\\
&\quad+\mu_{13}\langle\bar{B}_{6,v}\tilde{\chi}_+v^\mu S^\nu F^+_{\mu\nu}B_{\bar{3},v}+\text{H.c.}\rangle+\mu_{14}\langle\bar{B}_{\bar{3},v}\tilde{\chi}_+v^\mu S^\nu B_{\bar{3},v}\rangle\langle F^+_{\mu\nu}\rangle+\mu_{15}\langle\bar{B}_{6,v}\tilde{\chi}_+v^\mu S^\nu B_{6,v}\rangle\langle F^+_{\mu\nu}\rangle\\
&\quad+\mu_{16}\langle\bar{B}_{6,v}\tilde{\chi}_+v^\mu S^\nu B_{\bar{3},v}+\text{H.c.}\rangle\langle F^+_{\mu\nu}\rangle+\mu_{17}\langle\bar{B}_{\bar{3},v}v^\mu S^\nu F^+_{\mu\nu}B_{\bar{3},v}\rangle\langle\tilde{\chi}_+\rangle+\mu_{18}\langle\bar{B}_{6,v}v^\mu S^\nu F^+_{\mu\nu}B_{6,v}\rangle\langle\tilde{\chi}_+\rangle\\
&\quad+\mu_{19}\langle\bar{B}_{6,v}v^\mu S^\nu F^+_{\mu\nu}B_{\bar{3},v}+\text{H.c.}\rangle\langle\tilde{\chi}_+\rangle+\mu_{20}\langle\bar{B}_{\bar{3},v}v^\mu S^\nu B_{\bar{3},v}\rangle\langle\tilde{\chi}_+F^+_{\mu\nu}\rangle+\mu_{21}\langle\bar{B}_{6,v}v^\mu S^\nu B_{6,v}\rangle\langle\tilde{\chi}_+F^+_{\mu\nu}\rangle]+\ldots, \qquad (26)
\end{aligned}
$$

$$
\begin{aligned}
\mathcal{L}^{\text{eff}}_{\text{4qLR}} &= i\text{Re}(V_{ub})[\nu_1\langle\bar{B}_{\bar{3},v}\hat{\tilde{\chi}}_-B_{\bar{3},v}\rangle+\nu_2\langle\bar{B}_{6,v}\hat{\tilde{\chi}}_-B_{6,v}\rangle+\nu_3\langle\bar{B}_{6,v}\hat{\tilde{\chi}}_-B_{\bar{3},v}+\text{H.c.}\rangle+\nu_4\langle\bar{B}_{\bar{3},v}B_{\bar{3},v}\rangle\langle\hat{\tilde{\chi}}_-\rangle\\
&\quad+\nu_5\langle\bar{B}_{6,v}B_{6,v}\rangle\langle\hat{\tilde{\chi}}_-\rangle]+4i\text{Re}(V_{ub})[\nu_{11}\langle\bar{B}_{\bar{3},v}\hat{\tilde{\chi}}_+v^\mu S^\nu F^+_{\mu\nu}B_{\bar{3},v}\rangle+\nu_{12}\langle\bar{B}_{6,v}\hat{\tilde{\chi}}_+v^\mu S^\nu F^+_{\mu\nu}B_{6,v}\rangle\\
&\quad+\nu_{13}\langle\bar{B}_{6,v}\hat{\tilde{\chi}}_+v^\mu S^\nu F^+_{\mu\nu}B_{\bar{3},v}+\text{H.c.}\rangle+\nu_{14}\langle\bar{B}_{\bar{3},v}\hat{\tilde{\chi}}_+v^\mu S^\nu B_{\bar{3},v}\rangle\langle F^+_{\mu\nu}\rangle+\nu_{15}\langle\bar{B}_{6,v}\hat{\tilde{\chi}}_+v^\mu S^\nu B_{6,v}\rangle\langle F^+_{\mu\nu}\rangle\\
&\quad+\nu_{16}\langle\bar{B}_{6,v}\hat{\tilde{\chi}}_+v^\mu S^\nu B_{\bar{3},v}+\text{H.c.}\rangle\langle F^+_{\mu\nu}\rangle+\nu_{17}\langle\bar{B}_{\bar{3},v}v^\mu S^\nu F^+_{\mu\nu}B_{\bar{3},v}\rangle\langle\hat{\tilde{\chi}}_+\rangle+\nu_{18}\langle\bar{B}_{6,v}v^\mu S^\nu F^+_{\mu\nu}B_{6,v}\rangle\langle\hat{\tilde{\chi}}_+\rangle\\
&\quad+\nu_{19}\langle\bar{B}_{6,v}v^\mu S^\nu F^+_{\mu\nu}B_{\bar{3},v}+\text{H.c.}\rangle\langle\hat{\tilde{\chi}}_+\rangle+\nu_{20}\langle\bar{B}_{\bar{3},v}v^\mu S^\nu B_{\bar{3},v}\rangle\langle\hat{\tilde{\chi}}_+F^+_{\mu\nu}\rangle+\nu_{21}\langle\bar{B}_{6,v}v^\mu S^\nu B_{6,v}\rangle\langle\hat{\tilde{\chi}}_+F^+_{\mu\nu}\rangle].+\ldots. \qquad (27)
\end{aligned}
$$

We only display the terms which are relevant for the EDM calculation. Additionally, to the order at which we are working, only terms linear in the Goldstone bosons are needed. Terms that begin with more than a single Goldstone boson are hidden in the ellipses. Since the chiral singlet β^+ in the qCEDM Lagrangian can only enter as an overall constant, it is convenient to absorb β^+ into the LECs b_i.

Concerning the power counting rules of the CP-odd vertices, the chiral order of the sources is counted as $\mathcal{O}(\delta^0)$,

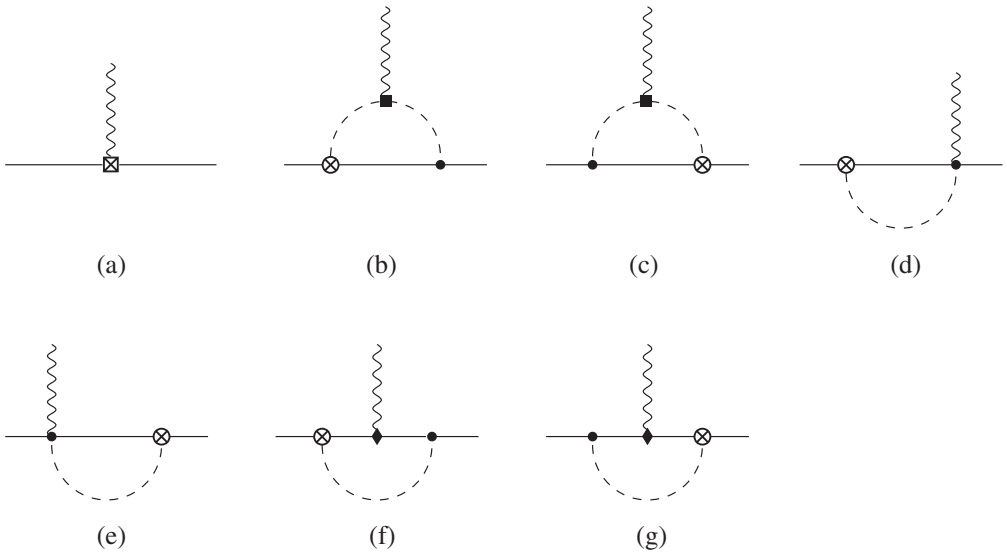

FIG. 1. Diagrams contributing to the EDMs of the spin-1/2 neutral antitriplet and sextet b baryons. Diagram (a) shows contact interactions and diagrams (b)–(g) one-loop corrections. Solid lines correspond to contribution from either spin-1/2 antitriplet or sextet multiplets of bottom baryons. Filled circles and squares are first-order meson-baryon and second-order mesonic vertices, respectively. While diamonds represent vertices generated by the first-order meson-baryon Lagrangian, CP-violating vertices at $\mathcal{O}(\delta^0)$ and $\mathcal{O}(\delta^2)$ are represented by crossed circle and crossed box, in order.

where δ is a generic small mass or momentum, since they do not contain any light scales and in addition will be common to all contributions considered in this work. For the remaining pieces, we employ standard chiral counting.

Figure 1 depicts the tree-level and one-loop Feynman diagrams that generate a nonvanishing contribution to the P- and T-violating form factor of the B_b baryons up to the order $\mathcal{O}(\delta^2)$. We evaluate the loop diagrams in the framework of dimensional regularization at the renormalization scale $\lambda = 1$ GeV. We apply the modified minimal subtraction scheme ($\widetilde{\text{MS}}$) in HBChPT [33–36] by absorbing the infinite parts in terms of

$$L = \frac{\lambda^{n-4}}{16\pi^2}\left[\frac{1}{n-4} + \frac{1}{2}(\gamma_E - 1 - \ln(4\pi))\right] \tag{28}$$

into the counterterms, with n the number of space-time dimensions and γ_E the Euler-Mascheroni constant. The tree-level CP-odd diagrams at order $\mathcal{O}(\delta^2)$ displayed in diagram (a) receive contributions from all the CP-violating operators. The one-loop diagrams at leading $\mathcal{O}(\delta^2)$ are given by diagrams (b)–(g) in Fig. 1.

IV. P- AND T-VIOLATING FORM FACTOR

The EDM of the neutral and charged b baryons can be extracted from the P- and T-violating form factor $D^{\gamma}_{B_b}(q^2)$. It is defined through

$$\langle B_b(p_f)|J_{\text{EDM},\nu}|B_b(p_i)\rangle = D^{\gamma}_{B_b}(q^2)\bar{u}(p_f)\sigma_{\mu\nu}\gamma_5 q^{\mu}u(p_i), \tag{29}$$

in the covariant formulation with momentum transfer $q = p_f - p_i$; see, e.g., Ref. [26]. The EDM is then given by

$$d^{\gamma}_{B_b} = D^{\gamma}_{B_b}(q^2 = 0). \tag{30}$$

One can reformulate the form factor in the heavy-baryon approach using the Breit frame. In this frame, we have $v \cdot p_i = v \cdot p_f$, and we set the 4-velocity to $v_{\mu} = (1, \mathbf{0})$. The form factor is then obtained as

$$\langle B_b(p_f)|J_{\text{EDM},\nu}|B_b(p_i)\rangle = -2iD^{\gamma}_{B_b}(q^2)\bar{B}_v v_{\nu}(S\cdot q)B_v. \tag{31}$$

We first consider the contributions from the tree-level diagrams in Fig. 1(a). The expressions of the electric dipole moment of the antitriplet and sextet b baryons from the

TABLE I. Tree-level contributions from the qEDM and qCEDM operators of the b baryons. Loop diagrams only appear at higher order.

Baryons	qEDM	qCEDM
Λ_b^0	$4c_1$	$-4eb_{19}$
Ξ_b^0	$4c_1$	$-4eb_{19}$
Ξ_b^-	$4c_1$	$-4e(b_{16}+b_{19})$
Σ_b^+	$2c_2$	$2e(b_{17}-b_{20})$
Σ_b^0	$2c_2$	$-2eb_{20}$
Σ_b^-	$2c_2$	$-2e(b_{17}+b_{20})$
$\Xi_b^{\prime 0}$	$2c_2$	$-2eb_{20}$
$\Xi_b^{\prime -}$	$2c_2$	$-2e(b_{17}+b_{20})$
Ω_b^-	$2c_2$	$-2e(b_{17}+b_{20})$

TABLE II. Tree-level contribution from the 4q operators of the b baryons. Loop diagrams appear at the same order.

Baryons	4q
Λ_b^0	$4e[\mu_{11}(\mu^{ub}-\mu^{db})-\mu_{14}(\mu^{ub}+\mu^{db})+2\mu_{20}(\mu^{ub}-\mu^{db}-\mu^{sb})]$
Ξ_b^0	$4e[\mu_{11}(\mu^{ub}-\mu^{sb})-\mu_{14}(\mu^{ub}+\mu^{sb})+2\mu_{20}(\mu^{ub}-\mu^{db}-\mu^{sb})]$
Ξ_b^-	$-4e[(\mu_{11}+\mu_{14})(\mu^{db}+\mu^{sb})+2\mu_{17}(\mu^{ub}+\mu^{db}+\mu^{sb})-2\mu_{20}(\mu^{ub}-\mu^{db}-\mu^{sb})]$
Σ_b^+	$4e[(\mu_{12}-\mu_{15})\mu^{ub}+\mu_{18}(\mu^{ub}+\mu^{db}+\mu^{sb})+\mu_{21}(\mu^{ub}-\mu^{db}-\mu^{sb})]$
Σ_b^0	$2e[\mu_{12}(\mu^{ub}-\mu^{db})-\mu_{15}(\mu^{ub}+\mu^{db})+2\mu_{21}(\mu^{ub}-\mu^{db}-\mu^{sb})]$
Σ_b^-	$-4e[(\mu_{12}+\mu_{15})\mu^{db}+\mu_{18}(\mu^{ub}+\mu^{db}+\mu^{sb})-\mu_{21}(\mu^{ub}-\mu^{db}-\mu^{sb})]$
$\Xi_b^{\prime 0}$	$2e[\mu_{12}(\mu^{ub}-\mu^{sb})-\mu_{15}(\mu^{ub}+\mu^{sb})+2\mu_{21}(\mu^{ub}-\mu^{db}-\mu^{sb})]$
$\Xi_b^{\prime -}$	$-2e[(\mu_{12}+\mu_{15})(\mu^{db}+\mu^{sb})+2\mu_{18}(\mu^{ub}+\mu^{db}+\mu^{sb})-2\mu_{21}(\mu^{ub}-\mu^{db}-\mu^{sb})]$
Ω_b^-	$-4e[(\mu_{12}+\mu_{15})\mu^{sb}+\mu_{18}(\mu^{ub}+\mu^{db}+\mu^{sb})-\mu_{21}(\mu^{ub}-\mu^{db}-\mu^{sb})]$

TABLE III. Tree-level contribution from 4qLR operators of the b baryons. Loop diagrams appear at the same order.

Baryons	4qLR
Λ_b^0	$4e\mathrm{Re}(V_{ub})(\nu_{11}-\nu_{14}+2\nu_{20})\nu^{ub}$
Ξ_b^0	$4e\mathrm{Re}(V_{ub})(\nu_{11}-\nu_{14}+2\nu_{20})\nu^{ub}$
Ξ_b^-	$-8e\mathrm{Re}(V_{ub})(\nu_{17}-\nu_{20})\nu^{ub}$
Σ_b^+	$4e\mathrm{Re}(V_{ub})(\nu_{12}-\nu_{15}+\nu_{18}+\nu_{21})\nu^{ub}$
Σ_b^0	$2e\mathrm{Re}(V_{ub})(\nu_{12}-\nu_{15}+2\nu_{21})\nu^{ub}$
Σ_b^-	$-4e\mathrm{Re}(V_{ub})(\nu_{18}-\nu_{21})\nu^{ub}$
$\Xi_b^{\prime 0}$	$2e\mathrm{Re}(V_{ub})(\nu_{12}-\nu_{15}+2\nu_{21})\nu^{ub}$
$\Xi_b^{\prime -}$	$-4e\mathrm{Re}(V_{ub})(\nu_{18}-\nu_{21})\nu^{ub}$
Ω_b^-	$-4e\mathrm{Re}(V_{ub})(\nu_{18}-\nu_{21})\nu^{ub}$

dimension-6 operators are collected in Tables I–III. In addition to the tree-level contributions, we find the one-loop diagrams in Fig. 1. In analogy to the neutron EDM, the EDMs of bottom baryons get contributions from the cloud of Goldstone bosons dressing the baryons. For the qEDM and qCEDM operators, the meson loops appear at higher order, and only the tree-level diagrams are necessary. But for the 4q and 4qLR operators, the loops appear at the same order, and the LECs of the tree-level contributions absorb the associated loop divergences.

We calculated the diagrams in Fig. 1 explicitly in heavy-baryon ChPT. We find that only diagrams (b) and (c) contribute at the order at which we work. The other diagrams are proportional to $S\cdot v=0$, or $v\cdot q=0$, or mutually cancel. The contributions from the nonvanishing diagrams can be written as

$$D_b^\gamma(q^2)=\frac{A_{b_i}}{2}\int_0^1 dx\,\frac{x}{\tilde{M}_i}\frac{\partial}{\partial\tilde{M}_i}J_1(\tilde{w},\tilde{M}_i),$$
$$D_c^\gamma(q^2)=\frac{A_{c_i}}{2}\int_0^1 dx\,\frac{x-1}{\tilde{M}_i}\frac{\partial}{\partial\tilde{M}_i}J_1(\tilde{w},\tilde{M}_i),\quad i=1,2,3,4, \tag{32}$$

where J_1 is the loop function defined in Appendix C, $\tilde{w}=-\Delta$ for a sextet particle inside the loop, or $\tilde{w}=0$ for an antitriplet particle. Furthermore, $\tilde{M}_i(x)=\sqrt{x(x-1)q^2+M_i^2}$, with M_i being $M_{K^\pm}$ or $M_{\pi^\pm}$. The coefficients A_{b_i} and A_{c_i} have to be determined from the vertices of the appearing interacting Lagrangians. A lot of these coefficients are similar to each other with some only differing by their sign. Considering isospin symmetry, this leads to additional cancellations when summing up the loop contributions. We refrain from showing the full list of coefficients A_{b_i} and A_{c_i} with their respective M_i here. The surviving terms together with their coefficients can be read off from the full form factor results listed in Appendix A.

The expressions for the complete form factors are given in Appendix A. Here, we present the results for the EDMs. For the 4q operator, we obtain

$$d^\gamma_{\Lambda_b^0,4q}=4e[\mu_{11}(\mu^{ub}-\mu^{db})-\mu_{14}(\mu^{ub}+\mu^{db})+2\mu_{20}(\mu^{ub}-\mu^{db}-\mu^{sb})]+\frac{eg_2\mu_8(\mu^{ub}+\mu^{sb})}{32\pi^2F_\pi^2}F^{(2)}_{M_K},$$
$$d^\gamma_{\Xi_b^0,4q}=4e[\mu_{11}(\mu^{ub}-\mu^{sb})-\mu_{14}(\mu^{ub}+\mu^{sb})+2\mu_{20}(\mu^{ub}-\mu^{db}-\mu^{sb})]+\frac{eg_2\mu_8(\mu^{ub}+\mu^{db})}{32\pi^2F_\pi^2}F^{(2)}_{M_\pi},$$
$$d^\gamma_{\Xi_b^-,4q}=-4e[(\mu_{11}+\mu_{14})(\mu^{db}+\mu^{sb})+2\mu_{17}(\mu^{ub}+\mu^{db}+\mu^{sb})-2\mu_{20}(\mu^{ub}-\mu^{db}-\mu^{sb})]$$
$$-\frac{eg_2\mu_8}{32\pi^2F_\pi^2}((\mu^{ub}+\mu^{sb})F^{(2)}_{M_K}+(\mu^{ub}+\mu^{db})F^{(2)}_{M_\pi}), \tag{33}$$

$$
\begin{aligned}
d^{\gamma}_{\Sigma_b^+,4\mathrm{q}} &= 4e[(\mu_{12}-\mu_{15})\mu^{ub}+\mu_{18}(\mu^{ub}+\mu^{db}+\mu^{sb})+\mu_{21}(\mu^{ub}-\mu^{db}-\mu^{sb})]\\
&\quad+\frac{eg_1\mu_7}{32\pi^2F_\pi^2}((\mu^{ub}+\mu^{sb})F^{(2)}_{M_K}+(\mu^{ub}+\mu^{db})F^{(2)}_{M_\pi})\\
&\quad+\frac{eg_2\mu_8}{16\pi^2F_\pi^2}((\mu^{ub}+\mu^{sb})F^{(1)}_{M_K}+(\mu^{ub}+\mu^{db})F^{(1)}_{M_\pi}),\\
d^{\gamma}_{\Sigma_b^0,4\mathrm{q}} &= 2e[\mu_{12}(\mu^{ub}-\mu^{db})-\mu_{15}(\mu^{ub}+\mu^{db})+2\mu_{21}(\mu^{ub}-\mu^{db}-\mu^{sb})]\\
&\quad+\frac{eg_1\mu_7(\mu^{ub}+\mu^{sb})}{64\pi^2F_\pi^2}F^{(2)}_{M_K}+\frac{eg_2\mu_8(\mu^{ub}+\mu^{sb})}{32\pi^2F_\pi^2}F^{(1)}_{M_K},\\
d^{\gamma}_{\Sigma_b^-,4\mathrm{q}} &= -4e[(\mu_{12}+\mu_{15})\mu^{db}+\mu_{18}(\mu^{ub}+\mu^{db}+\mu^{sb})-\mu_{21}(\mu^{ub}-\mu^{db}-\mu^{sb})]\\
&\quad-\frac{eg_1\mu_7(\mu^{ub}+\mu^{db})}{32\pi^2F_\pi^2}F^{(2)}_{M_\pi}-\frac{eg_2\mu_8(\mu^{ub}+\mu^{db})}{16\pi^2F_\pi^2}F^{(1)}_{M_\pi},\\
d^{\gamma}_{\Xi_b^0,4\mathrm{q}} &= 2e[\mu_{12}(\mu^{ub}-\mu^{sb})-\mu_{15}(\mu^{ub}+\mu^{sb})+2\mu_{21}(\mu^{ub}-\mu^{db}-\mu^{sb})]\\
&\quad+\frac{eg_1\mu_7(\mu^{ub}+\mu^{db})}{64\pi^2F_\pi^2}F^{(2)}_{M_\pi}+\frac{eg_2\mu_8(\mu^{ub}+\mu^{db})}{32\pi^2F_\pi^2}F^{(1)}_{M_\pi},\\
d^{\gamma}_{\Xi_b'^-,4\mathrm{q}} &= -2e[(\mu_{12}+\mu_{15})(\mu^{db}+\mu^{sb})+2\mu_{18}(\mu^{ub}+\mu^{db}+\mu^{sb})-2\mu_{21}(\mu^{ub}-\mu^{db}-\mu^{sb})]\\
&\quad-\frac{eg_1\mu_7}{64\pi^2F_\pi^2}((\mu^{ub}+\mu^{sb})F^{(2)}_{M_K}+(\mu^{ub}+\mu^{db})F^{(2)}_{M_\pi})\\
&\quad-\frac{eg_2\mu_8}{32\pi^2F_\pi^2}((\mu^{ub}+\mu^{sb})F^{(1)}_{M_K}+(\mu^{ub}+\mu^{db})F^{(1)}_{M_\pi}),\\
d^{\gamma}_{\Omega_b^-,4\mathrm{q}} &= -4e[(\mu_{12}+\mu_{15})\mu^{sb}+\mu_{18}(\mu^{ub}+\mu^{db}+\mu^{sb})-\mu_{21}(\mu^{ub}-\mu^{db}-\mu^{sb})]\\
&\quad-\frac{eg_1\mu_7(\mu^{ub}+\mu^{sb})}{32\pi^2F_\pi^2}F^{(2)}_{M_K}-\frac{eg_2\mu_8(\mu^{ub}+\mu^{sb})}{16\pi^2F_\pi^2}F^{(1)}_{M_K}.
\end{aligned}
\tag{34}
$$

For the 4qLR operator, we obtain

$$
\begin{aligned}
d^{\gamma}_{\Lambda_b^0,4qLR} &= 4e\mathrm{Re}(V_{ub})(\nu_{11}-\nu_{14}+2\nu_{20})\nu^{ub}+\frac{e\mathrm{Re}(V_{ub})g_2\nu_3\nu^{ub}}{32\pi^2F_\pi^2}F^{(2)}_{M_K},\\
d^{\gamma}_{\Xi_b^0,4\mathrm{qLR}} &= 4e\mathrm{Re}(V_{ub})(\nu_{11}-\nu_{14}+2\nu_{20})\nu^{ub}+\frac{e\mathrm{Re}(V_{ub})g_2\nu_3\nu^{ub}}{32\pi^2F_\pi^2}F^{(2)}_{M_\pi},\\
d^{\gamma}_{\Xi_b^-,4\mathrm{qLR}} &= -8e\mathrm{Re}(V_{ub})(\nu_{17}-\nu_{20})\nu^{ub}-\frac{e\mathrm{Re}(V_{ub})g_2\nu_3\nu^{ub}}{32\pi^2F_\pi^2}(F^{(2)}_{M_K}+F^{(2)}_{M_\pi}),\\
d^{\gamma}_{\Sigma_b^+,4\mathrm{qLR}} &= 4e\mathrm{Re}(V_{ub})(\nu_{12}-\nu_{15}+\nu_{18}+\nu_{21})\nu^{ub}+\frac{e\mathrm{Re}(V_{ub})g_1\nu_2\nu^{ub}}{32\pi^2F_\pi^2}(F^{(2)}_{M_K}+F^{(2)}_{M_\pi})+\frac{e\mathrm{Re}(V_{ub})g_2\nu_3\nu^{ub}}{16\pi^2F_\pi^2}(F^{(1)}_{M_K}+F^{(1)}_{M_\pi}),
\end{aligned}
\tag{35}
$$

$$
\begin{aligned}
d^{\gamma}_{\Sigma_b^0,4\mathrm{qLR}} &= 2e\mathrm{Re}(V_{ub})(\nu_{12}-\nu_{15}+2\nu_{21})\nu^{ub}+\frac{e\mathrm{Re}(V_{ub})g_1\nu_2\nu^{ub}}{64\pi^2F_\pi^2}F^{(2)}_{M_K}+\frac{e\mathrm{Re}(V_{ub})g_2\nu_3\nu^{ub}}{32\pi^2F_\pi^2}F^{(1)}_{M_K},\\
d^{\gamma}_{\Sigma_b^-,4\mathrm{qLR}} &= -4e\mathrm{Re}(V_{ub})(\nu_{18}-\nu_{21})\nu^{ub}-\frac{e\mathrm{Re}(V_{ub})g_1\nu_2\nu^{ub}}{32\pi^2F_\pi^2}F^{(2)}_{M_\pi}-\frac{e\mathrm{Re}(V_{ub})g_2\nu_3\nu^{ub}}{16\pi^2F_\pi^2}F^{(1)}_{M_\pi},\\
d^{\gamma}_{\Xi_b'^0,4\mathrm{qLR}} &= 2e\mathrm{Re}(V_{ub})(\nu_{12}-\nu_{15}+2\nu_{21})\nu^{ub}+\frac{e\mathrm{Re}(V_{ub})g_1\nu_2\nu^{ub}}{64\pi^2F_\pi^2}F^{(2)}_{M_\pi}+\frac{e\mathrm{Re}(V_{ub})g_2\nu_3\nu^{ub}}{32\pi^2F_\pi^2}F^{(1)}_{M_\pi},\\
d^{\gamma}_{\Xi_b'^-,4\mathrm{qLR}} &= -4e\mathrm{Re}(V_{ub})(\nu_{18}-\nu_{21})\nu^{ub}-\frac{e\mathrm{Re}(V_{ub})g_1\nu_2\nu^{ub}}{64\pi^2F_\pi^2}(F^{(2)}_{M_K}+F^{(2)}_{M_\pi})-\frac{e\mathrm{Re}(V_{ub})g_2\nu_3\nu^{ub}}{32\pi^2F_\pi^2}(F^{(1)}_{M_K}+F^{(1)}_{M_\pi}),\\
d^{\gamma}_{\Omega_b^-,4\mathrm{qLR}} &= -4e\mathrm{Re}(V_{ub})(\nu_{18}-\nu_{21})\nu^{ub}-\frac{e\mathrm{Re}(V_{ub})g_1\nu_2\nu^{ub}}{32\pi^2F_\pi^2}F^{(2)}_{M_K}-\frac{e\mathrm{Re}(V_{ub})g_2\nu_3\nu^{ub}}{16\pi^2F_\pi^2}F^{(1)}_{M_K},
\end{aligned}
\tag{36}
$$

where the loop functions are defined as

$$F^{(1)}_{M_\pi} = 1 + 32\pi^2 L + 2\ln\left[\frac{M_\pi}{\lambda}\right],$$
$$F^{(2)}_{M_\pi} = 1 + 32\pi^2 L + 2\ln\left[\frac{M_\pi}{\lambda}\right] + \frac{2\Delta}{\sqrt{\Delta^2 - M_\pi^2}}\ln\left[\frac{\Delta}{M_\pi} + \sqrt{\frac{\Delta^2}{M_\pi^2} - 1}\right],$$
$$F^{(1)}_{M_K} = 1 + 32\pi^2 L + 2\ln\left[\frac{M_K}{\lambda}\right],$$
$$F^{(2)}_{M_K} = 1 + 32\pi^2 L + 2\ln\left[\frac{M_K}{\lambda}\right] + \frac{2\Delta\arccos[\frac{\Delta}{M_K}]}{\sqrt{M_K^2 - \Delta^2}}. \quad (37)$$

A. Patterns of EDMs

Before discussing the absolute sizes of the EDMs in the next section, we investigate the relative sizes of the various EDMs. The relative sizes are essentially determined by the chiral symmetry properties and field content of the underlying sources of CP violation. For instance, for the bottom qEDM at the order at which we work, the EDMs of all baryons in the triplet or the sextet are determined by a single LEC, c_1 and c_2, in order. This pattern is different for the qCEDM where in the triplet $d_{\Xi_b^-}$ is expected to be different from $d^\gamma_{\Lambda_b^0} = d^\gamma_{\Xi_b^0}$. Similarly, in the sextet, we obtain the relations for the qCEDM $d^\gamma_{\Sigma_b^-} + d^\gamma_{\Sigma_b^+} = 2d^\gamma_{\Sigma_b^0}$, which are also true for the qEDM, but $d^\gamma_{\Sigma_b^-} \neq d^\gamma_{\Sigma_b^+}$. These differences arise because in order for the qCEDM to generate an EDM of a baryon an insertion of the quark charge is required. As such, EDMs of baryons with a single b quark but different charges differ for the qCEDM. This is not true for the bottom qEDM as the operator already contains a photon.

A richer pattern emerges for the four-quark operators as here loop diagrams provide leading contributions. For instance, for the 4qLR, we observe that the tree-level contributions to the triplet and sextet EDMs have pattern identical to that of the qCEDM. However, the loop contributions induce differences. In the triplet, loop contributions lead to a splitting in the EDMs of the neutral baryons and $d^\gamma_{\Lambda_b^0} \neq d^\gamma_{\Xi_b^0}$, because of the different Goldstone bosons participating in the loops. We find

$$d^\gamma_{\Lambda_b^0,\mathrm{4qLR}} - d^\gamma_{\Xi_b^0,\mathrm{4qLR}} = \frac{e\mathrm{Re}(V_{ub})g_2\nu_3\nu^{ub}}{16\pi^2 F_\pi^2}\left(2\ln\frac{M_K}{M_\pi} + \frac{2\Delta\arccos[\frac{\Delta}{M_K}]}{\sqrt{M_K^2 - \Delta^2}} - \frac{2\Delta}{\sqrt{\Delta^2 - M_\pi^2}}\ln\left[\frac{\Delta}{M_\pi} + \sqrt{\frac{\Delta^2}{M_\pi^2} - 1}\right]\right), \quad (38)$$

which is nonzero and finite, whereas for the qCEDM, this combination vanishes. In the same way, the degeneracy that is present for the qCEDM for the negatively charged sextet baryons is broken by the 4qLR operator. To illustrate this, while for both the qCEDM and the 4qLR we have $d^\gamma_{\Xi_b'^-} - (d^\gamma_{\Sigma_b^-} + d^\gamma_{\Omega_b^-})/2 = 0$, only for the 4qLR, $d^\gamma_{\Sigma_b^-} - d^\gamma_{\Omega_b^-} \neq 0$ (and finite).

Finally, for the 4q operators, an even different pattern of EDMs arises depending on the flavor configuration of the underlying operator. From Eqs. (15) and (19), it is clear that the chiral symmetry properties of μ^{ub} are identical to the 4qLR operator $\sim\nu^{ub}$. As such, for μ^{ub}, the same pattern of EDMs emerges as for the 4qLR, and these sources cannot be separated from symmetry arguments alone. Different patterns do emerge for μ^{db} and μ^{sb}. For example, the splitting in the triplet is different for μ^{db} with respect to the 4qLR, but this can probably only be used with additional information on the LECs.

The above considerations indicate that the pattern of EDMs of bottom baryons provide information about the source of CP violation. If experiments, for instance, those proposed in Refs. [14–16], were to see nonzero signals, this information could be used to pinpoint the underlying mechanism. Much more could be said with nonperturbative information about the LECs appearing in the Lagrangians.

V. HOW LARGE ARE THE EDMs?

To determine the sizes of the EDMs of bottom baryons as function of the various dimension-6 Wilson coefficients appearing in Eq. (1), estimates of the various LECs appearing in EDM expressions are necessary. This requires nonperturbative QCD calculations of the associated matrix elements. While a lot of progress has been made in this direction for EDMs of systems containing first-generation quarks, see, e.g., Ref. [37] for a recent review, as far as we know, no calculations have been performed for baryons containing heavier valence quarks. In this work, we estimate the contributions using naive dimensional analysis (NDA), a technique discussed in detail in Refs. [38,39] and used for nucleon EDMs in Ref. [4]. While NDA does not give accurate predictions, it provides a reasonable order-of-magnitude estimate for meson and single-baryon matrix elements and is the guiding principle for a systematic power counting in effective field theories.

The EDMs of the bottom baryons under consideration depend, for each source of CP violation, on several LECs. The easiest estimates are for the bottom EDM. NDA predicts

$$c_{1,2} = \mathcal{O}(d_b) = \mathcal{O}\left(\frac{m_b}{\Lambda^2}\right), \quad (39)$$

which is a rather intuitive result. The bottom-quark EDM operator directly induces a bottom-baryon EDM up to order-1 factors. The factors could be calculated with nonperturbative methods such as lattice QCD or estimated using a quark model. For light quarks, for instance, lattice QCD predicts the neutron EDM to be $d_n = 0.82 d_d - 0.21 d_u$ [40] in agreement with NDA estimates.

Next, we consider the qCEDM. In this case, we need to estimate the LECs $b_{16} - b_{20}$. NDA predicts

$$b_{16-20} = \mathcal{O}\left(\tilde{d}_b \frac{F_\pi}{\Lambda_\chi}\right) = \mathcal{O}\left(\frac{F_\pi m_b}{\Lambda_\chi \Lambda^2}\right), \tag{40}$$

where we used $4\pi F_\pi \sim \Lambda_\chi$. The loop diagrams only contribute at next-to-next-to-leading order. It would be interesting to compare these predictions with other estimates, for instance, through QCD sum rules.

For the four-quark operators, we need to estimate both the tree-level LECs and the CP-odd Goldstone boson-baryon interactions. For the $4q$ terms, we obtain

$$\begin{aligned} \mu_{6-10}\mu^{qb} &= \mathcal{O}(\mu^{qb}\Lambda_\chi F_\pi^2) = \mathcal{O}\left(\frac{\Lambda_\chi F_\pi^2}{\Lambda^2}\right), \\ \mu_{11-21}\mu^{qb} &= \mathcal{O}\left(e\mu^{qb}\frac{F_\pi^2}{\Lambda_\chi}\right) = \mathcal{O}\left(e\frac{F_\pi^2}{\Lambda_\chi \Lambda^2}\right), \end{aligned} \tag{41}$$

where $q = \{u, d, s\}$. While the Goldstone boson-baryon terms scale as $\sim\Lambda_\chi^1$, and are thus of lower order than the EDM vertices $\sim\Lambda_\chi^{-1}$, they only contribute to the EDMs at the one-loop level bringing in a loop factor $e/(4\pi F_\pi)^2 \sim e\Lambda_\chi^{-2}$ so that both types of vertices contribute at the same order.

Similarly for the 4qLR operator, we obtain

$$\begin{aligned} \nu_{1-5}\nu^{ub} &= \mathcal{O}(\nu^{ub}\Lambda_\chi F_\pi^2) = \mathcal{O}\left(\frac{\Lambda_\chi F_\pi^2}{\Lambda^2}\right), \\ \nu_{11-21}\nu^{ub} &= \mathcal{O}\left(e\nu^{ub}\frac{F_\pi^2}{\Lambda_\chi}\right) = \mathcal{O}\left(e\frac{F_\pi^2}{\Lambda_\chi \Lambda^2}\right). \end{aligned} \tag{42}$$

While the NDA estimates are rough, they give a reasonable idea of the scale of BSM physics that can be probed by measuring EDMs of bottom baryons with a given sensitivity. For instance, for a BSM physics scale,[1] $\Lambda = 1$ TeV, and considering only the tree-level expressions, we estimate

$$d^\gamma_{B_b} = \{10^{-19}, 10^{-20}, 10^{-21}, 10^{-24}\}\ e\,\mathrm{cm}, \tag{43}$$

for the qEDM, qCEDM, 4q, and 4qLR operators, respectively. The smallness of the last term is explained by the factor of $\mathrm{Re}(V_{ub})$. These estimates involve a sizeable uncertainty. Nevertheless, they can be used to determine the reach of a potential program to measure the EDMs of bottom-quark baryons. To get an idea of the uncertainty, we used a Monte Carlo (MC) sampling of the LECs that appear in the EDM expressions. For instance, for the qEDM operator, we rescaled the LECs

$$c_{1,2} \to \left(\frac{m_b}{\Lambda^2}\right)\tilde{c}_{1,2} \tag{44}$$

and varied the dimensionless constants $\tilde{c}_{1,2}$ between $[-3, +3]$. After the MC sampling, we obtained a list of different values for the qEDM contribution from which we computed the mean value and the standard deviation. We used this procedure for all LECs appearing in the EDM expression and obtained the mean values and standard deviations for the various EDMs for each CP-odd source in Tables IV and V. The MC method is just a tool to determine roughly in what range we can expect an EDM for the various sources at a given scale Λ.

In Table IV, we collect the different contributions to the EDMs of the antitriplet states. For each source, we get, unsurprisingly, results that vary around zero with a spread given by the NDA estimates. There is roughly an order-of-magnitude uncertainty. As expected, the qEDM dominates, whereas the 4qLR term gives the smallest contribution. The standard deviations for all contributions are relatively large, which is explained by the wide range of the dimensionless constants which was used in the MC sampling. The same observations can also be drawn from Table V. In the case in which all four dimension-6 operators contribute at the same BSM scale Λ, we can take a look at the resulting size of the EDM by adding up the single contributions. Taking the Ω_b^- baryon as an example, the total EDM would be

TABLE IV. Numerical contributions to the EDMs of the antitriplet baryons for $\Lambda = 1$ TeV. The results are given in 10^{-19} , 10^{-20} , 10^{-21} , and 10^{-24} e cm for the qEDM, qCEDM, 4q, and 4qLR operators, respectively.

Contribution	Λ_b^0	Ξ_b^0	Ξ_b^-
qEDM	-0.24 ± 5.7	-0.24 ± 5.7	-0.24 ± 5.7
qCEDM	$+0.18 \pm 4.6$	$+0.18 \pm 4.6$	$+0.40 \pm 6.5$
4q	-0.070 ± 2.4	-0.020 ± 2.5	$+0.040 \pm 3.2$
4qLR	$+0.15 \pm 9.4$	$+0.58 \pm 9.6$	-0.11 ± 10.8

[1]This scale is comparable to indirect limits obtained from traditional EDM experiments. For example, a b-quark EDM mixes with a b-quark CEDM under the one-loop QED renormalization group. At the b-quark threshold, the latter induces a Weinberg three-gluon operator [10], which, in turn, induces a neutron EDM. Based on this procedure, Ref. [12] quotes an indirect limit $d_b < 1.2 \times 10^{-2}$ e cm. Using our parametrization $d_b = m_b/\Lambda^2$, we get $\Lambda > 2$ TeV. However, this indirect limit suffers from a large theoretical uncertainty due to the poorly known neutron EDM matrix element of the Weinberg operator [11,13]. Furthermore, the neutron EDM can get contributions from other sources. We therefore consider $\Lambda = 1$ TeV as a reasonable and pragmatic choice.

TABLE V. Numerical contributions to the EDMs of the sextet baryons for $\Lambda = 1$ TeV. The results are given in 10^{-19} , 10^{-20} , 10^{-21} , and 10^{-24} e cm for the qEDM, qCEDM, 4q, and 4qLR operators, respectively.

Contribution	Σ_b^+	Σ_b^0	Σ_b^-	$\Xi_b'^0$	$\Xi_b'^-$	Ω_b^-
qEDM	-0.16 ± 2.8	-0.16 ± 2.8	-0.16 ± 2.8	-0.1 ± 2.8	-0.16 ± 2.8	-0.16 ± 2.8
qCEDM	$+0.10 \pm 3.3$	$+0.04 \pm 2.2$	$+0.070 \pm 3.3$	$+0.040 \pm 2.2$	$+0.070 \pm 3.3$	$+0.070 \pm 3.3$
4q	-0.050 ± 2.1	$+0.070 \pm 1.2$	$+0.040 \pm 2.1$	$+0.020 \pm 1.3$	$+0.050 \pm 1.6$	-0.060 ± 2.0
4qLR	-0.23 ± 7.9	-0.010 ± 4.9	$+0.21 \pm 5.7$	$+0.050 \pm 4.8$	$+0.21 \pm 5.6$	$+0.35 \pm 5.3$

$$d^{\gamma}_{\Omega_b^-} = (-0.15 \pm 3.2) \times 10^{-19} (\mathrm{TeV}/\Lambda)^2 \; e\,\mathrm{cm}. \quad (45)$$

This value is, of course, not to be understood as a clear prediction but as an estimate for the range where the EDM of the Ω_b^- baryon can be found. The experiment would involve the positively charged antibaryons (e.g., Ω_b^+) whose EDMs are the same as the corresponding baryons by CPT. The errors here reflect the uncertainty on the hadronic theory, and while the error band includes zero, nothing would indicate a vanishing matrix element. For the qEDM and qCEDM operators, indirect limits have been set from the EDM of the neutron and diamagnetic atoms [10–13]. We do not compare these limits here in detail as the indirect limits are plagued by sizeable uncertainties as well (mainly from matrix elements connecting the three-gluon Weinberg operator to the neutron EDM) and assume that there are not other contributions to the neutron EDM (for instance, from EDMs or CEDMs of light quarks). Our main goal here is to assess the reach of a potential experimental program to measure the EDMs of bottom-quark baryons.

VI. CONCLUSION

Electric dipole moment experiments provide one of the most sensitive searches for BSM physics. Most focus has been on EDMs of stable systems consisting of first-generation quarks, but it has been proposed to look for EDMs of baryons containing heavier quarks as well [14–16]. Such systems are sensitive to CP-odd operators involving second- and third-generation quarks and complement existing searches. However, essentially no theoretical calculations have been performed to guide this developing experimental program.

In this paper, we have analyzed the EDMs of spin-1/2 baryons containing a single bottom quark. Our starting point has been operators of dimension 6 in the SMEFT Lagrangian that violate CP and contain a $\bar{b}\Gamma b$ bilinear (where Γ denotes a Lorentz structure). We considered a hypothetical bottom-quark EDM and chromo-EDM and several four-quark operators mixing bottom quarks with lighter quarks. We used chiral perturbation theory to construct the resulting CP-violating hadronic interactions between spin-1/2 single-bottom baryons, Goldstone bosons, and photons and calculated the EDMs up to the first nonvanishing order for each source of CP violation.

Our results indicate that different sources of CP violation lead to a different pattern of EDMs due to the chiral- and isospin-symmetry properties of the underlying sources. In principle, this would allow for the identification of the dominant source of CP violation based on the relative sizes of EDMs of triplet and sextet bottom-quark baryons. The absolute sizes of the EDMs, however, are very uncertain, as very little is known about the magnitudes of the low-energy constants appearing in the CP-odd chiral Lagrangian. We made estimates using naive dimensional analysis and found that for BSM scales of 1 TeV we can expect EDMs in the range of $10^{-19} - 10^{-24}$ e cm depending strongly on the dimension-6 operators under consideration. All EDMs scale as Λ^{-2}, so the sizes of the EDMs can easily be obtained for other BSM scales. If the experimental program picks up steam and EDMs of these systems are targeted, it would be good to calculate the LECs with nonperturbative techniques to get more reliable estimates. The techniques developed in this work can be readily extended to calculate EDMs of charmed baryons, and work along these lines is in progress.

ACKNOWLEDGMENTS

Partial financial support from the DFG (Project No. 196253076-TRR 110) and the NSFC (Grant No. 11621131001) through the funds provided to the Sino-German CRC 110 "Symmetries and the Emergence of Structure in QCD"; by the Chinese Academy of Sciences (CAS) through a President's International Fellowship Initiative (PIFI) (Grant No. 2018DM0034); by the VolkswagenStiftung (Grant No. 93562); and by the EU Horizon 2020 research and innovation programme, STRONG-2020 project (Grant No. 824093) is acknowledged.

APPENDIX A: FORM FACTORS

The full expression for the neutral and charged b-baryon form factors up to the order $\mathcal{O}(\delta^2)$ with the tree-level results is

$$
\begin{aligned}
D^{\gamma}_{\Lambda_b^0}(q^2) &= 4c_1 - 4e(b_{19} - \mu_{11}(\mu^{ub} - \mu^{db}) + \mu_{14}(\mu^{ub} + \mu^{db}) - 2\mu_{20}(\mu^{ub} - \mu^{db} - \mu^{sb}) \\
&\quad - \mathrm{Re}(V_{ub})(\nu_{11} - \nu_{14} + 2\nu_{20})\nu^{ub}) \\
&\quad + \frac{eg_2}{4F_\pi^2}(\mathrm{Re}(V_{ub})\nu_3\nu^{ub} + \mu_8(\mu^{ub} + \mu^{sb}))\int_0^1 dx \frac{1}{\tilde{M}_K}\frac{\partial}{\partial \tilde{M}_K} J_1(-\Delta, \tilde{M}_K), \\
D^{\gamma}_{\Xi_b^0}(q^2) &= 4c_1 - 4e(b_{19} - \mu_{11}(\mu^{ub} - \mu^{sb}) + \mu_{14}(\mu^{ub} + \mu^{sb}) - 2\mu_{20}(\mu^{ub} - \mu^{db} - \mu^{sb}) \\
&\quad - \mathrm{Re}(V_{ub})(\nu_{11} - \nu_{14} + 2\nu_{20})\nu^{ub}) \\
&\quad + \frac{eg_2}{4F_\pi^2}(\mathrm{Re}(V_{ub})\nu_3\nu^{ub} + \mu_8(\mu^{ub} + \mu^{db}))\int_0^1 dx \frac{1}{\tilde{M}_\pi}\frac{\partial}{\partial \tilde{M}_\pi} J_1(-\Delta, \tilde{M}_\pi), \\
D^{\gamma}_{\Xi_b^-}(q^2) &= 4c_1 - 4e(b_{16} + b_{19} + (\mu_{11} + \mu_{14})(\mu^{db} + \mu^{sb}) + 2\mu_{17}(\mu^{ub} + \mu^{db} + \mu^{sb}) \\
&\quad - 2\mu_{20}(\mu^{ub} - \mu^{db} - \mu^{sb}) + 2\mathrm{Re}(V_{ub})(\nu_{17} - \nu_{20})\nu^{ub}) \\
&\quad - \frac{eg_2}{4\pi^2 F_\pi^2}(\mathrm{Re}(V_{ub})\nu_3\nu^{ub} + \mu_8(\mu^{ub} + \mu^{sb}))\int_0^1 dx \frac{1}{\tilde{M}_K}\frac{\partial}{\partial \tilde{M}_K} J_1(-\Delta, \tilde{M}_K) \\
&\quad - \frac{eg_2}{4\pi^2 F_\pi^2}(\mathrm{Re}(V_{ub})\nu_3\nu^{ub} + \mu_8(\mu^{ub} + \mu^{db}))\int_0^1 dx \frac{1}{\tilde{M}_\pi}\frac{\partial}{\partial \tilde{M}_\pi} J_1(-\Delta, \tilde{M}_\pi), \\
D^{\gamma}_{\Sigma_b^+}(q^2) &= 2c_2 + 2e(b_{17} - b_{20} + 2(\mu_{12} - \mu_{15})\mu^{ub} + 2\mu_{18}(\mu^{ub} + \mu^{db} + \mu^{sb}) \\
&\quad + 2\mu_{21}(\mu^{ub} - \mu^{db} - \mu^{sb}) + 2\mathrm{Re}(V_{ub})(\nu_{12} - \nu_{15} + \nu_{18} + \nu_{21})\nu^{ub}) \\
&\quad + \frac{eg_1}{4\pi^2 F_\pi^2}(\mathrm{Re}(V_{ub})\nu_2\nu^{ub} + \mu_7(\mu^{ub} + \mu^{sb}))\int_0^1 dx \frac{1}{\tilde{M}_K}\frac{\partial}{\partial \tilde{M}_K} J_1(-\Delta, \tilde{M}_K) \\
&\quad + \frac{eg_1}{4\pi^2 F_\pi^2}(\mathrm{Re}(V_{ub})\nu_2\nu^{ub} + \mu_7(\mu^{ub} + \mu^{db}))\int_0^1 dx \frac{1}{\tilde{M}_\pi}\frac{\partial}{\partial \tilde{M}_\pi} J_1(-\Delta, \tilde{M}_\pi) \\
&\quad + \frac{eg_2}{2\pi^2 F_\pi^2}(\mathrm{Re}(V_{ub})\nu_3\nu^{ub} + \mu_8(\mu^{ub} + \mu^{sb}))\int_0^1 dx \frac{1}{\tilde{M}_K}\frac{\partial}{\partial \tilde{M}_K} J_1(0, \tilde{M}_K) \\
&\quad + \frac{eg_2}{2\pi^2 F_\pi^2}(\mathrm{Re}(V_{ub})\nu_3\nu^{ub} + \mu_8(\mu^{ub} + \mu^{db}))\int_0^1 dx \frac{1}{\tilde{M}_\pi}\frac{\partial}{\partial \tilde{M}_\pi} J_1(0, \tilde{M}_\pi), \\
D^{\gamma}_{\Sigma_b^0}(q^2) &= 2c_2 - 2e(b_{20} - \mu_{12}(\mu^{ub} - \mu^{db}) + \mu_{15}(\mu^{ub} + \mu^{db}) - 2\mu_{21}(\mu^{ub} - \mu^{db} - \mu^{sb}) \\
&\quad - \mathrm{Re}(V_{ub})(\nu_{12} - \nu_{15} + 2\nu_{21})\nu^{ub}) \\
&\quad + \frac{eg_1}{8F_\pi^2}(\mathrm{Re}(V_{ub})\nu_2\nu^{ub} + \mu_7(\mu^{ub} + \mu^{sb}))\int_0^1 dx \frac{1}{\tilde{M}_K}\frac{\partial}{\partial \tilde{M}_K} J_1(-\Delta, \tilde{M}_K) \\
&\quad + \frac{eg_2}{4F_\pi^2}(\mathrm{Re}(V_{ub})\nu_3\nu^{ub} + \mu_8(\mu^{ub} + \mu^{sb}))\int_0^1 dx \frac{1}{\tilde{M}_K}\frac{\partial}{\partial \tilde{M}_K} J_1(0, \tilde{M}_K), \\
D^{\gamma}_{\Sigma_b^-}(q^2) &= 2c_2 - 2e(b_{17} + b_{20} + 2(\mu_{12} + \mu_{15})\mu^{db} + 2\mu_{18}(\mu^{ub} + \mu^{db} + \mu^{sb}) \\
&\quad - 2\mu_{21}(\mu^{ub} - \mu^{db} - \mu^{sb}) + 2\mathrm{Re}(V_{ub})(\nu_{18} - \nu_{21})\nu^{ub}) \\
&\quad - \frac{eg_1}{4\pi^2 F_\pi^2}(\mathrm{Re}(V_{ub})\nu_2\nu^{ub} + \mu_7(\mu^{ub} + \mu^{db}))\int_0^1 dx \frac{1}{\tilde{M}_\pi}\frac{\partial}{\partial \tilde{M}_\pi} J_1(-\Delta, \tilde{M}_\pi) \\
&\quad - \frac{eg_2}{2\pi^2 F_\pi^2}(\mathrm{Re}(V_{ub})\nu_3\nu^{ub} + \mu_8(\mu^{ub} + \mu^{db}))\int_0^1 dx \frac{1}{\tilde{M}_\pi}\frac{\partial}{\partial \tilde{M}_\pi} J_1(0, \tilde{M}_\pi), \\
D^{\gamma}_{\Xi_b'^0}(q^2) &= 2c_2 - 2e(b_{20} - \mu_{12}(\mu^{ub} - \mu^{sb}) + \mu_{15}(\mu^{ub} + \mu^{sb}) - 2\mu_{21}(\mu^{ub} - \mu^{db} - \mu^{sb}) \\
&\quad - \mathrm{Re}(V_{ub})(\nu_{12} - \nu_{15} + 2\nu_{21})\nu^{ub})
\end{aligned}
$$

$$
\begin{aligned}
&+\frac{eg_1}{8F_\pi^2}(\mathrm{Re}(V_{ub})\nu_2\nu^{ub}+\mu_7(\mu^{ub}+\mu^{db}))\int_0^1 dx\frac{1}{\tilde{M}_\pi}\frac{\partial}{\partial\tilde{M}_\pi}J_1(-\Delta,\tilde{M}_\pi)\\
&+\frac{eg_2}{4F_\pi^2}(\mathrm{Re}(V_{ub})\nu_3\nu^{ub}+\mu_8(\mu^{ub}+\mu^{db}))\int_0^1 dx\frac{1}{\tilde{M}_\pi}\frac{\partial}{\partial\tilde{M}_\pi}J_1(0,\tilde{M}_\pi),\\
D^\gamma_{\Xi_b'^-}(q^2)=&\,2c_2-2e(b_{17}+b_{20}+(\mu_{12}+\mu_{15})(\mu^{db}+\mu^{sb})+2\mu_{18}(\mu^{ub}+\mu^{db}+\mu^{sb})\\
&-2\mu_{21}(\mu^{ub}-\mu^{db}-\mu^{sb})+2\mathrm{Re}(V_{ub})(\nu_{18}-\nu_{21})\nu^{ub})\\
&-\frac{eg_1}{8\pi^2F_\pi^2}(\mathrm{Re}(V_{ub})\nu_2\nu^{ub}+\mu_7(\mu^{ub}+\mu^{sb}))\int_0^1 dx\frac{1}{\tilde{M}_K}\frac{\partial}{\partial\tilde{M}_K}J_1(-\Delta,\tilde{M}_K)\\
&-\frac{eg_1}{8\pi^2F_\pi^2}(\mathrm{Re}(V_{ub})\nu_2\nu^{ub}+\mu_7(\mu^{ub}+\mu^{db}))\int_0^1 dx\frac{1}{\tilde{M}_\pi}\frac{\partial}{\partial\tilde{M}_\pi}J_1(-\Delta,\tilde{M}_\pi)\\
&-\frac{eg_2}{4\pi^2F_\pi^2}(\mathrm{Re}(V_{ub})\nu_3\nu^{ub}+\mu_8(\mu^{ub}+\mu^{sb}))\int_0^1 dx\frac{1}{\tilde{M}_K}\frac{\partial}{\partial\tilde{M}_K}J_1(0,\tilde{M}_K)\\
&-\frac{eg_2}{4\pi^2F_\pi^2}(\mathrm{Re}(V_{ub})\nu_3\nu^{ub}+\mu_8(\mu^{ub}+\mu^{db}))\int_0^1 dx\frac{1}{\tilde{M}_\pi}\frac{\partial}{\partial\tilde{M}_\pi}J_1(0,\tilde{M}_\pi),\\
D^\gamma_{\Omega_b^-}(q^2)=&\,2c_2-2e(b_{17}+b_{20}+2(\mu_{12}+\mu_{15})\mu^{sb}+2\mu_{18}(\mu^{ub}+\mu^{db}+\mu^{sb})\\
&-2\mu_{21}(\mu^{ub}-\mu^{db}-\mu^{sb})+2\mathrm{Re}(V_{ub})(\nu_{18}-\nu_{21})\nu^{ub})\\
&-\frac{eg_1}{4\pi^2F_\pi^2}(\mathrm{Re}(V_{ub})\nu_2\nu^{ub}+\mu_7(\mu^{ub}+\mu^{sb}))\int_0^1 dx\frac{1}{\tilde{M}_K}\frac{\partial}{\partial\tilde{M}_K}J_1(-\Delta,\tilde{M}_K)\\
&-\frac{eg_2}{2\pi^2F_\pi^2}(\mathrm{Re}(V_{ub})\nu_3\nu^{ub}+\mu_8(\mu^{ub}+\mu^{sb}))\int_0^1 dx\frac{1}{\tilde{M}_K}\frac{\partial}{\partial\tilde{M}_K}J_1(0,\tilde{M}_K).
\end{aligned}
\tag{A1}
$$

APPENDIX B: EDMS WITH NDA ESTIMATES

Replacing the unknown LECs in the equations for the neutral and charged b-baryon EDMs with the NDA estimate leads to the expressions

$$
\begin{aligned}
d^\gamma_{\Lambda_b^0}=&\,4\left(\frac{m_b}{\Lambda^2}\right)\tilde{c}_1-4e\left(\frac{m_b}{4\pi\Lambda^2}\right)\tilde{b}_{19}+4e\left(\frac{F_\pi}{4\pi\Lambda^2}\right)[\tilde{\mu}_{11}-\tilde{\mu}_{14}+2\tilde{\mu}_{20}+\mathrm{Re}(V_{ub})(\tilde{\nu}_{11}-\tilde{\nu}_{14}+2\tilde{\nu}_{20})]\\
&+\frac{eg_2}{32\pi^2}\frac{\Lambda_\chi}{\Lambda^2}(\mathrm{Re}(V_{ub})\tilde{\nu}_3+\tilde{\mu}_8)\left(1+2\ln\left[\frac{M_K}{\lambda}\right]+\frac{2\Delta\mathrm{Arccos}[\frac{\Delta}{M_K}]}{\sqrt{M_K^2-\Delta^2}}\right),\\
d^\gamma_{\Xi_b^0}=&\,4\left(\frac{m_b}{\Lambda^2}\right)\tilde{c}_1-4e\left(\frac{m_b}{4\pi\Lambda^2}\right)\tilde{b}_{19}+4e\left(\frac{F_\pi}{4\pi\Lambda^2}\right)[\tilde{\mu}_{11}-\tilde{\mu}_{14}+2\tilde{\mu}_{20}+\mathrm{Re}(V_{ub})(\tilde{\nu}_{11}-\tilde{\nu}_{14}+2\tilde{\nu}_{20})]\\
&+\frac{eg_2}{32\pi^2}\frac{\Lambda_\chi}{\Lambda^2}(\mathrm{Re}(V_{ub})\tilde{\nu}_3+\tilde{\mu}_8)\left(1+2\ln\left[\frac{M_\pi}{\lambda}\right]+\frac{2\Delta}{\sqrt{\Delta^2-M_\pi^2}}\ln\left[\frac{\Delta}{M_\pi}+\sqrt{\frac{\Delta^2}{M_\pi^2}-1}\right]\right),\\
d^\gamma_{\Xi_b^-}=&\,4\left(\frac{m_b}{\Lambda^2}\right)\tilde{c}_1-4e\left(\frac{m_b}{4\pi\Lambda^2}\right)(\tilde{b}_{16}+\tilde{b}_{19})\\
&-4e\left(\frac{F_\pi}{4\pi\Lambda^2}\right)[\tilde{\mu}_{11}+\tilde{\mu}_{14}+2\tilde{\mu}_{17}-2\tilde{\mu}_{20}+2\mathrm{Re}(V_{ub})(\tilde{\nu}_{17}-\tilde{\nu}_{20})]-\frac{eg_2}{32\pi^2}\frac{\Lambda_\chi}{\Lambda^2}(\mathrm{Re}(V_{ub})\tilde{\nu}_3+\tilde{\mu}_8)\\
&\times\left(2+2\ln\left[\frac{M_K}{\lambda}\right]+\frac{2\Delta\mathrm{Arccos}[\frac{\Delta}{M_K}]}{\sqrt{M_K^2-\Delta^2}}+2\ln\left[\frac{M_\pi}{\lambda}\right]+\frac{2\Delta}{\sqrt{\Delta^2-M_\pi^2}}\ln\left[\frac{\Delta}{M_\pi}+\sqrt{\frac{\Delta^2}{M_\pi^2}-1}\right]\right),
\end{aligned}
$$

$$
\begin{aligned}
d^{\gamma}_{\Sigma_b^+} &= 2\left(\frac{m_b}{\Lambda^2}\right)\tilde{c}_2 + 2e\left(\frac{m_b}{4\pi\Lambda^2}\right)(\tilde{b}_{17}-\tilde{b}_{20}) \\
&\quad + 4e\left(\frac{F_\pi}{4\pi\Lambda^2}\right)[\tilde{\mu}_{12}-\tilde{\mu}_{15}+\tilde{\mu}_{18}+\tilde{\mu}_{21}+\mathrm{Re}(V_{ub})(\tilde{\nu}_{12}-\tilde{\nu}_{15}+\tilde{\nu}_{18}+\tilde{\nu}_{21})] \\
&\quad + \frac{eg_2}{16\pi^2}\frac{\Lambda_\chi}{\Lambda^2}(\mathrm{Re}(V_{ub})\tilde{\nu}_3+\tilde{\mu}_8)\left(2+2\ln\left[\frac{M_K M_\pi}{\lambda^2}\right]\right) + \frac{eg_1}{32\pi^2}\frac{\Lambda_\chi}{\Lambda^2}(\mathrm{Re}(V_{ub})\tilde{\nu}_2+\tilde{\mu}_7) \\
&\quad \times\left(2+2\ln\left[\frac{M_K}{\lambda}\right]+\frac{2\Delta\mathrm{Arccos}[\frac{\Delta}{M_K}]}{\sqrt{M_K^2-\Delta^2}}+2\ln\left[\frac{M_\pi}{\lambda}\right]+\frac{2\Delta}{\sqrt{\Delta^2-M_\pi^2}}\ln\left[\frac{\Delta}{M_\pi}+\sqrt{\frac{\Delta^2}{M_\pi^2}-1}\right]\right), \\
d^{\gamma}_{\Sigma_b^0} &= 2\left(\frac{m_b}{\Lambda^2}\right)\tilde{c}_2 - 2e\left(\frac{m_b}{4\pi\Lambda^2}\right)\tilde{b}_{20} + 2e\left(\frac{F_\pi}{4\pi\Lambda^2}\right)[\tilde{\mu}_{12}-\tilde{\mu}_{15}+2\tilde{\mu}_{21}+\mathrm{Re}(V_{ub})(\tilde{\nu}_{12}-\tilde{\nu}_{15}+2\tilde{\nu}_{21})] \\
&\quad + \frac{eg_1}{64\pi^2}\frac{\Lambda_\chi}{\Lambda^2}(\mathrm{Re}(V_{ub})\tilde{\nu}_2+\tilde{\mu}_7)\left(1+2\ln\left[\frac{M_K}{\lambda}\right]+\frac{2\Delta\mathrm{Arccos}[\frac{\Delta}{M_K}]}{\sqrt{M_K^2-\Delta^2}}\right) \\
&\quad + \frac{eg_2}{32\pi^2}\frac{\Lambda_\chi}{\Lambda^2}(\mathrm{Re}(V_{ub})\tilde{\nu}_3+\tilde{\mu}_8)\left(1+2\ln\left[\frac{M_K}{\lambda}\right]\right), \\
d^{\gamma}_{\Sigma_b^-} &= 2\left(\frac{m_b}{\Lambda^2}\right)\tilde{c}_2 - 2e\left(\frac{m_b}{4\pi\Lambda^2}\right)(\tilde{b}_{17}+\tilde{b}_{20}) - 4e\left(\frac{F_\pi}{4\pi\Lambda^2}\right)[\tilde{\mu}_{12}+\tilde{\mu}_{15}+\tilde{\mu}_{18}-\tilde{\mu}_{21}+\mathrm{Re}(V_{ub})(\tilde{\nu}_{18}-\tilde{\nu}_{21})] \\
&\quad - \frac{eg_1}{32\pi^2}\frac{\Lambda_\chi}{\Lambda^2}(\mathrm{Re}(V_{ub})\tilde{\nu}_2+\tilde{\mu}_7)\left(1+2\ln\left[\frac{M_\pi}{\lambda}\right]+\frac{2\Delta}{\sqrt{\Delta^2-M_\pi^2}}\ln\left[\frac{\Delta}{M_\pi}+\sqrt{\frac{\Delta^2}{M_\pi^2}-1}\right]\right) \\
&\quad - \frac{eg_2}{16\pi^2}\frac{\Lambda_\chi}{\Lambda^2}(\mathrm{Re}(V_{ub})\tilde{\nu}_3+\tilde{\mu}_8)\left(1+2\ln\left[\frac{M_\pi}{\lambda}\right]\right), \\
d^{\gamma}_{\Xi_b'^0} &= 2\left(\frac{m_b}{\Lambda^2}\right)\tilde{c}_2 - 2e\left(\frac{m_b}{4\pi\Lambda^2}\right)\tilde{b}_{20} + 2e\left(\frac{F_\pi}{4\pi\Lambda^2}\right)[\tilde{\mu}_{12}-\tilde{\mu}_{15}+2\tilde{\mu}_{21}+\mathrm{Re}(V_{ub})(\tilde{\nu}_{12}-\tilde{\nu}_{15}+2\tilde{\nu}_{21})] \\
&\quad + \frac{eg_1}{64\pi^2}\frac{\Lambda_\chi}{\Lambda^2}(\mathrm{Re}(V_{ub})\tilde{\nu}_2+\tilde{\mu}_7)\left(1+2\ln\left[\frac{M_\pi}{\lambda}\right]+\frac{2\Delta}{\sqrt{\Delta^2-M_\pi^2}}\ln\left[\frac{\Delta}{M_\pi}+\sqrt{\frac{\Delta^2}{M_\pi^2}-1}\right]\right) \\
&\quad + \frac{eg_2}{32\pi^2}\frac{\Lambda_\chi}{\Lambda^2}(\mathrm{Re}(V_{ub})\tilde{\nu}_3+\tilde{\mu}_8)\left(1+2\ln\left[\frac{M_\pi}{\lambda}\right]\right), \\
d^{\gamma}_{\Xi_b'^-} &= 2\left(\frac{m_b}{\Lambda^2}\right)\tilde{c}_2 - 2e\left(\frac{m_b}{4\pi\Lambda^2}\right)(\tilde{b}_{17}+\tilde{b}_{20}) - 2e\left(\frac{F_\pi}{4\pi\Lambda^2}\right)[\tilde{\mu}_{12}+\tilde{\mu}_{15}+2\tilde{\mu}_{18}-2\tilde{\mu}_{21}+2\mathrm{Re}(V_{ub})(\tilde{\nu}_{18}-\tilde{\nu}_{21})] \\
&\quad - \frac{eg_2}{32\pi^2}\frac{\Lambda_\chi}{\Lambda^2}(\mathrm{Re}(V_{ub})\tilde{\nu}_3+\tilde{\mu}_8)\left(2+2\ln\left[\frac{M_K M_\pi}{\lambda^2}\right]\right) - \frac{eg_1}{64\pi^2}\frac{\Lambda_\chi}{\Lambda^2}(\mathrm{Re}(V_{ub})\tilde{\nu}_2+\tilde{\mu}_7) \\
&\quad \times\left(2+2\ln\left[\frac{M_K}{\lambda}\right]+\frac{2\Delta\mathrm{Arccos}[\frac{\Delta}{M_K}]}{\sqrt{M_K^2-\Delta^2}}+2\ln\left[\frac{M_\pi}{\lambda}\right]+\frac{2\Delta}{\sqrt{\Delta^2-M_\pi^2}}\ln\left[\frac{\Delta}{M_\pi}+\sqrt{\frac{\Delta^2}{M_\pi^2}-1}\right]\right), \\
d^{\gamma}_{\Omega_b^-} &= 2\left(\frac{m_b}{\Lambda^2}\right)\tilde{c}_2 - 2e\left(\frac{m_b}{4\pi\Lambda^2}\right)(\tilde{b}_{17}+\tilde{b}_{20}) - 4e\left(\frac{F_\pi}{4\pi\Lambda^2}\right)[\tilde{\mu}_{12}+\tilde{\mu}_{15}+\tilde{\mu}_{18}-\tilde{\mu}_{21}+\mathrm{Re}(V_{ub})(\tilde{\nu}_{18}-\tilde{\nu}_{21})] \\
&\quad - \frac{eg_1}{32\pi^2}\frac{\Lambda_\chi}{\Lambda^2}(\mathrm{Re}(V_{ub})\tilde{\nu}_2+\tilde{\mu}_7)\left(1+2\ln\left[\frac{M_K}{\lambda}\right]+\frac{2\Delta\mathrm{Arccos}[\frac{\Delta}{M_K}]}{\sqrt{M_K^2-\Delta^2}}\right) \\
&\quad - \frac{eg_2}{16\pi^2}\frac{\Lambda_\chi}{\Lambda^2}(\mathrm{Re}(V_{ub})\tilde{\nu}_3+\tilde{\mu}_8)\left(1+2\ln\left[\frac{M_K}{\lambda}\right]\right),
\end{aligned}
\tag{B1}
$$

where $\tilde{c}_i$, $\tilde{b}_i$, $\tilde{\mu}_i$, and $\tilde{\nu}_i$ are dimensionless constants which are varied from -3 to $+3$ in the MC sampling. The estimation $4\pi F_\pi \sim \Lambda_\chi$ has been used at certain steps.

APPENDIX C: LOOP FUNCTIONS

In this Appendix, we give the loop functions in the heavy-baryon formulation [41] which appear in the calculation of the diagrams in Fig. 1,

$$\Delta_M = 2M^2\left[L + \frac{1}{16\pi^2}\ln\left(\frac{M}{\lambda}\right)\right] + \mathcal{O}(n-4),$$
$$\frac{1}{i}\int \frac{d^nk}{(2\pi)^n}\frac{1}{M^2-k^2} = \Delta_M = M^{n-2}(4\pi)^{-n/2}\Gamma\left(1-\frac{n}{2}\right), \tag{C1}$$

$$\frac{1}{i}\int \frac{d^nk}{(2\pi)^n}\frac{\{1, k_\mu, k_\mu k_\nu\}}{[v\cdot k - w][M^2-k^2]} = \{J_0(w), v_\mu J_1(w), g_{\mu\nu}J_2(w) + v_\mu v_\nu J_3(w)\}, \tag{C2}$$

$$\frac{1}{i}\int \frac{d^nk}{(2\pi)^n}\frac{\{1, k_\mu, k_\mu k_\nu\}}{[v\cdot k - w]^2[M^2-k^2]} = \{G_0(w), v_\mu G_1(w), g_{\mu\nu}G_2(w) + v_\mu v_\nu G_3(w)\}, \tag{C3}$$

$$\frac{1}{i}\int \frac{d^nk}{(2\pi)^n}\frac{1}{[v\cdot k - w)][M^2-k^2][(k+q)^2-M^2]} = \int_0^1 dx \frac{1}{2\tilde{M}}\frac{\partial}{\partial\tilde{M}}J_0(\tilde{w},\tilde{M}), \tag{C4}$$

$$\frac{1}{i}\int \frac{d^nk}{(2\pi)^n}\frac{k_\mu}{[v\cdot k - w][M^2-k^2][(k+q)^2-M^2]} = \int_0^1 dx\left(\frac{v_\mu}{2\tilde{M}}\frac{\partial}{\partial\tilde{M}}J_1(\tilde{w},\tilde{M}) - \frac{xq_\mu}{2\tilde{M}}\frac{\partial}{\partial\tilde{M}}J_0(\tilde{w},\tilde{M})\right), \tag{C5}$$

$$\frac{1}{i}\int \frac{d^nk}{(2\pi)^n}\frac{k_\mu k_\nu}{[v\cdot k - w][M^2-k^2][(k+q)^2-M^2]}$$
$$= \int_0^1 dx\left(\frac{g_{\mu\nu}}{2\tilde{M}}\frac{\partial}{\partial\tilde{M}}J_2(\tilde{w},\tilde{M}) + \frac{v_\mu v_\nu}{2\tilde{M}}\frac{\partial}{\partial\tilde{M}}J_3(\tilde{w},\tilde{M}) - (q_\mu v_\nu + q_\nu v_\mu)\frac{x}{2\tilde{M}}\frac{\partial}{\partial\tilde{M}}J_1(\tilde{w},\tilde{M}) + \frac{x^2q_\mu q_\nu}{2\tilde{M}}\frac{\partial}{\partial\tilde{M}}J_0(\tilde{w},\tilde{M})\right), \tag{C6}$$

where $\tilde{w}(x) = w + xv\cdot q$ and $\tilde{M}^2(x) = x(x-1)q^2 + M^2$. The analytical expressions for the loop functions in dimensional regularization are

$$J_0(w) = -4Lw + \frac{w}{8\pi^2}\left[1 - 2\ln\left(\frac{M}{\lambda}\right)\right] - \frac{1}{4\pi^2}\sqrt{M^2-w^2}\,\mathrm{ArcCos}\left(\frac{-w}{M}\right) + \mathcal{O}(n-4) \tag{C7}$$

for $M^2 > w^2$,

$$J_0(w) = -4Lw + \frac{w}{8\pi^2}\left[1 - 2\ln\left(\frac{M}{\lambda}\right)\right] + \frac{1}{4\pi^2}\sqrt{w^2-M^2}\ln\left(\frac{-w}{M} + \sqrt{\frac{w^2}{M^2}-1}\right) + \mathcal{O}(n-4) \tag{C8}$$

for $w^2 > M^2$, and

$$J_1(w) = wJ_0(w) + \Delta_M, \qquad J_2(w) = \frac{1}{n-1}[(M^2-w^2)J_0(w) - w\Delta_M], \tag{C9}$$

$$J_3(w) = wJ_1(w) - J_2(w), \tag{C10}$$

$$G_i(w) = \frac{\partial}{\partial w}J_i(w), \quad i = 0,1,2,3. \tag{C11}$$

[1] C. Abel *et al.* (nEDM Collaboration), Phys. Rev. Lett. **124**, 081803 (2020).
[2] W. C. Griffith, M. D. Swallows, T. H. Loftus, M. V. Romalis, B. R. Heckel, and E. N. Fortson, Phys. Rev. Lett. **102**, 101601 (2009).
[3] B. Grzadkowski, M. Iskrzynski, M. Misiak, and J. Rosiek, J. High Energy Phys. 10 (2010) 085.
[4] J. de Vries, R. G. E. Timmermans, E. Mereghetti, and U. van Kolck, Phys. Lett. B **695**, 268 (2011).
[5] J. de Vries, E. Mereghetti, R. G. E. Timmermans, and U. van Kolck, Ann. Phys. (Amsterdam) **338**, 50 (2013).
[6] J. Bsaisou, U.-G. Meißner, A. Nogga, and A. Wirzba, Ann. Phys. (Amsterdam) **359**, 317 (2015).
[7] N. Yamanaka and E. Hiyama, Phys. Rev. D **103**, 035023 (2021).
[8] J. Kley, T. Theil, E. Venturini, and A. Weiler, arXiv:2109.15085.
[9] W. Dekens, J. de Vries, J. Bsaisou, W. Bernreuther, C. Hanhart, U.-G. Meißner, A. Nogga, and A. Wirzba, J. High Energy Phys. 07 (2014) 069.
[10] E. Braaten, C. S. Li, and T. C. Yuan, Phys. Rev. D **42**, 276 (1990).
[11] Y. T. Chien, V. Cirigliano, W. Dekens, J. de Vries, and E. Mereghetti, J. High Energy Phys. 02 (2016) 011.
[12] H. Gisbert and J. Ruiz Vidal, Phys. Rev. D **101**, 115010 (2020),
[13] U. Haisch and G. Koole, J. High Energy Phys. 09 (2021) 133.
[14] A. S. Fomin *et al.*, J. High Energy Phys. 08 (2017) 120.
[15] S. Aiola *et al.*, Phys. Rev. D **103**, 072003 (2021).
[16] E. Bagli *et al.*, Eur. Phys. J. C **77**, 828 (2017); **80**, 680(E) (2020).
[17] Y. Ünal and U.-G. Meißner, J. High Energy Phys. 01 (2021) 115.
[18] J. Bsaisou, Ph.D. thesis, Bonn U., 2014.
[19] Y. Nakai and M. Reece, J. High Energy Phys. 08 (2017) 031.
[20] M. Jung and A. Pich, J. High Energy Phys. 04 (2014) 076.
[21] W. Dekens, J. de Vries, M. Jung, and K. K. Vos, J. High Energy Phys. 01 (2019) 069.
[22] H.-Y. Cheng, C.-Y. Cheung, G.-L. Lin, Y. C. Lin, T.-M. Yan, and H.-L. Yu, Phys. Rev. D **49**, 5857 (1994); **55**, 5851(E) (1997).
[23] T.-M. Yan, H.-Y. Cheng, C.-Y. Cheung, G.-L. Lin, Y. C. Lin, and H.-L. Yu, Phys. Rev. D **46**, 1148 (1992); **55**, 5851(E) (1997).
[24] R.-X. Shi, Y. Xiao, and L.-S. Geng, Phys. Rev. D **100**, 054019 (2019).
[25] N. Jiang, X.-L. Chen, and S.-L. Zhu, Phys. Rev. D **90**, 074011 (2014).
[26] B. Borasoy, Phys. Rev. D **61**, 114017 (2000).
[27] F.-K. Guo, C. Hanhart, and U.-G. Meißner, J. High Energy Phys. 09 (2008) 136.
[28] N. Jiang, X.-L. Chen, and S.-L. Zhu, Phys. Rev. D **92**, 054017 (2015).
[29] U.-G. Meißner and S. Steininger, Nucl. Phys. **B499**, 349 (1997).
[30] B. Kubis and U.-G. Meißner, Eur. Phys. J. C **18**, 747 (2001).
[31] E. E. Jenkins and A. V. Manohar, Phys. Lett. B **255**, 558 (1991).
[32] V. Bernard, N. Kaiser, J. Kambor, and U.-G. Meißner, Nucl. Phys. **B388**, 315 (1992).
[33] G. 't Hooft, Nucl. Phys. **B61**, 455 (1973).
[34] S. Weinberg, Phys. Rev. D **8**, 3497 (1973).
[35] J. Gasser and H. Leutwyler, Ann. Phys. (N.Y.) **158**, 142 (1984).
[36] S. Scherer and M. R. Schindler, Lect. Notes Phys. **830**, 1 (2012).
[37] A. Shindler, Eur. Phys. J. A **57**, 128 (2021).
[38] S. Weinberg, Phys. Rev. Lett. **63**, 2333 (1989).
[39] A. Manohar and H. Georgi, Nucl. Phys. **B234**, 189 (1984).
[40] T. Bhattacharya, V. Cirigliano, R. Gupta, H.-W. Lin, and B. Yoon, Phys. Rev. Lett. **115**, 212002 (2015).
[41] V. Bernard, N. Kaiser, and U.-G. Meißner, Int. J. Mod. Phys. E **4**, 193 (1995).